

COSMIC MAGNETIC FIELDS

KRZYSZTOF NALEWAJKO, CAMK PAN

KNALEW@CAMK.EDU.PL

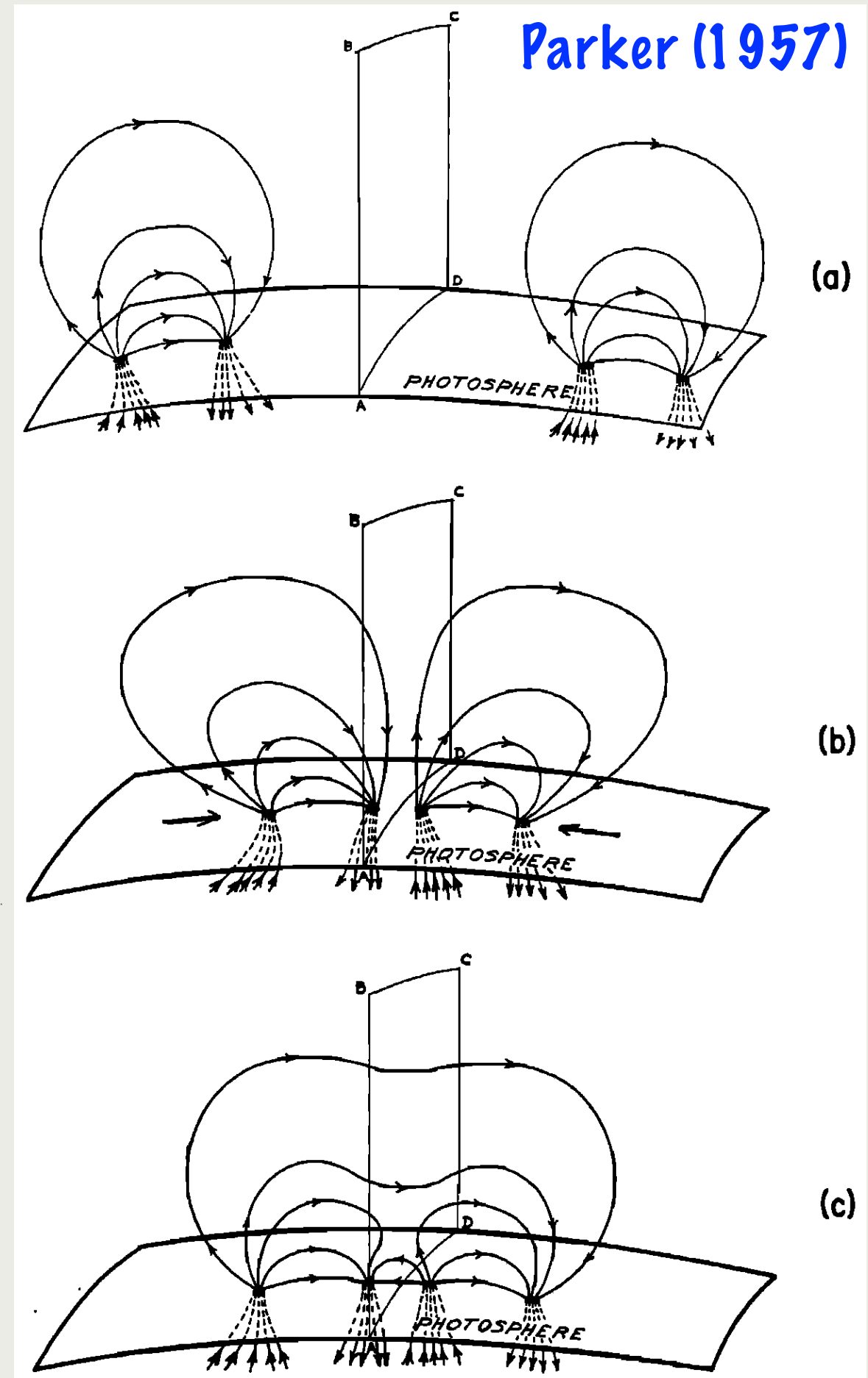
Magnetic reconnection

PROPOSITION OF MAGNETIC RECONNECTION

A mechanism is proposed here for the production of these flares based on the energies acquired by charged particles moving in induced electric fields associated with sunspots.

Apart from a general magnetic field, fields from other sunspots may still be of appreciable size in the neighbourhood of the spot under consideration. It is thus to be expected that there will be places where actual neutral points exist and where conditions are thus suitable for the excitation of atoms by collision.

Giovanelli (1946)

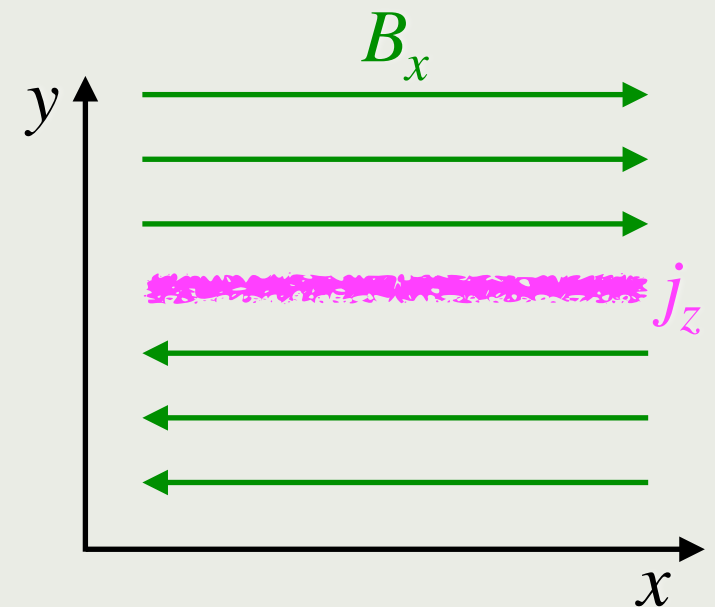


CURRENT LAYER (SHEET)

- Consider an interface of thickness δ between anti-parallel magnetic fields:

$$B_x \simeq B_0 \text{ for } y > \delta/2,$$

$$B_x \simeq -B_0 \text{ for } y < -\delta/2.$$



- The magnetic field gradient $\partial_y B_x = (4\pi/c)j_z \sim B_0/\delta$ implies a current density $j_z \sim cB_0/4\pi\delta$ in the layer.
- The magnetic pressure $P_{yy} \sim B_0^2/8\pi$ has a gap in the layer that can be supported by gas pressure (or sheared B_z field component).

HARRIS EQUILIBRIUM

- 1D equilibrium with anti-parallel asymptotically flat B-field

$$B_x = B_0 \tanh(y/\delta)$$

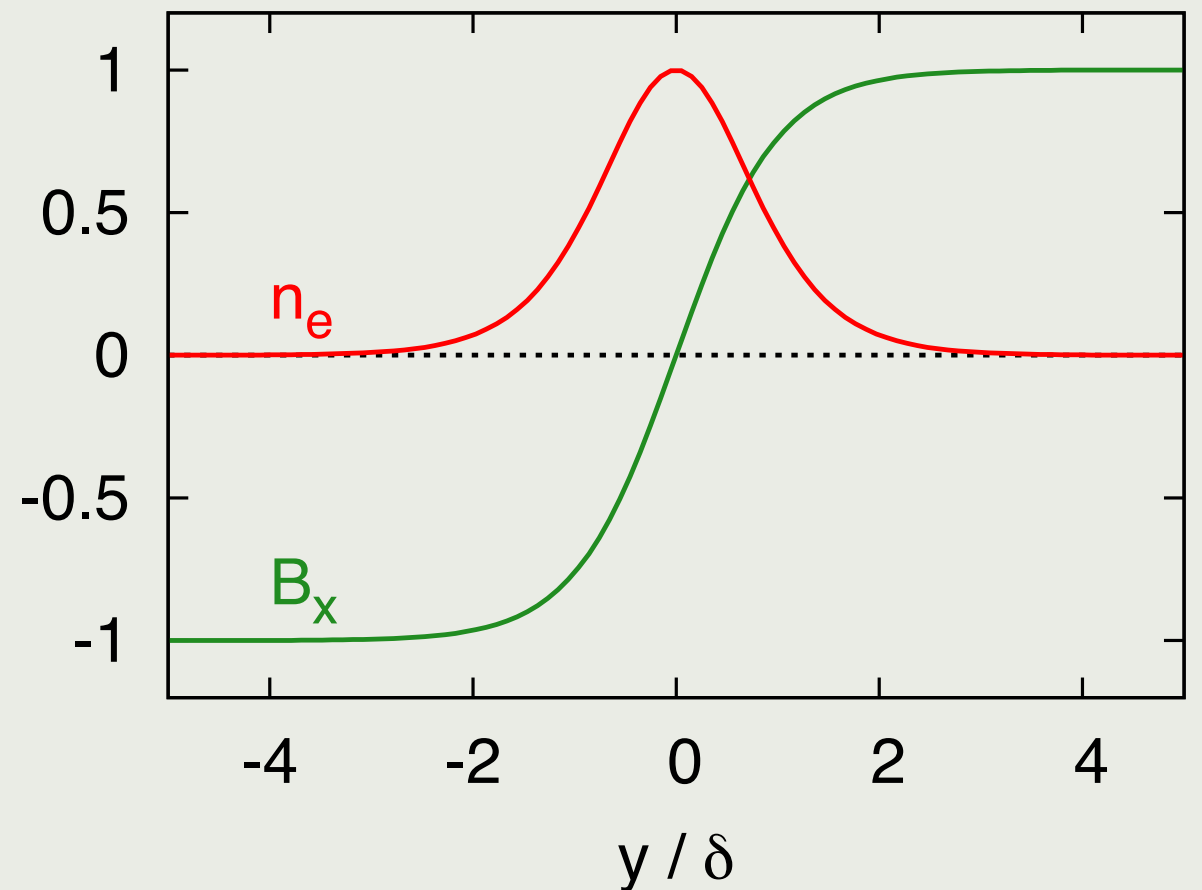
- population of hot drifting particles to provide current density and pressure support

$$n = n_d / \cosh^2(y/\delta)$$

- uniform background plasma n_0 or guide field B_z do not affect the equilibrium

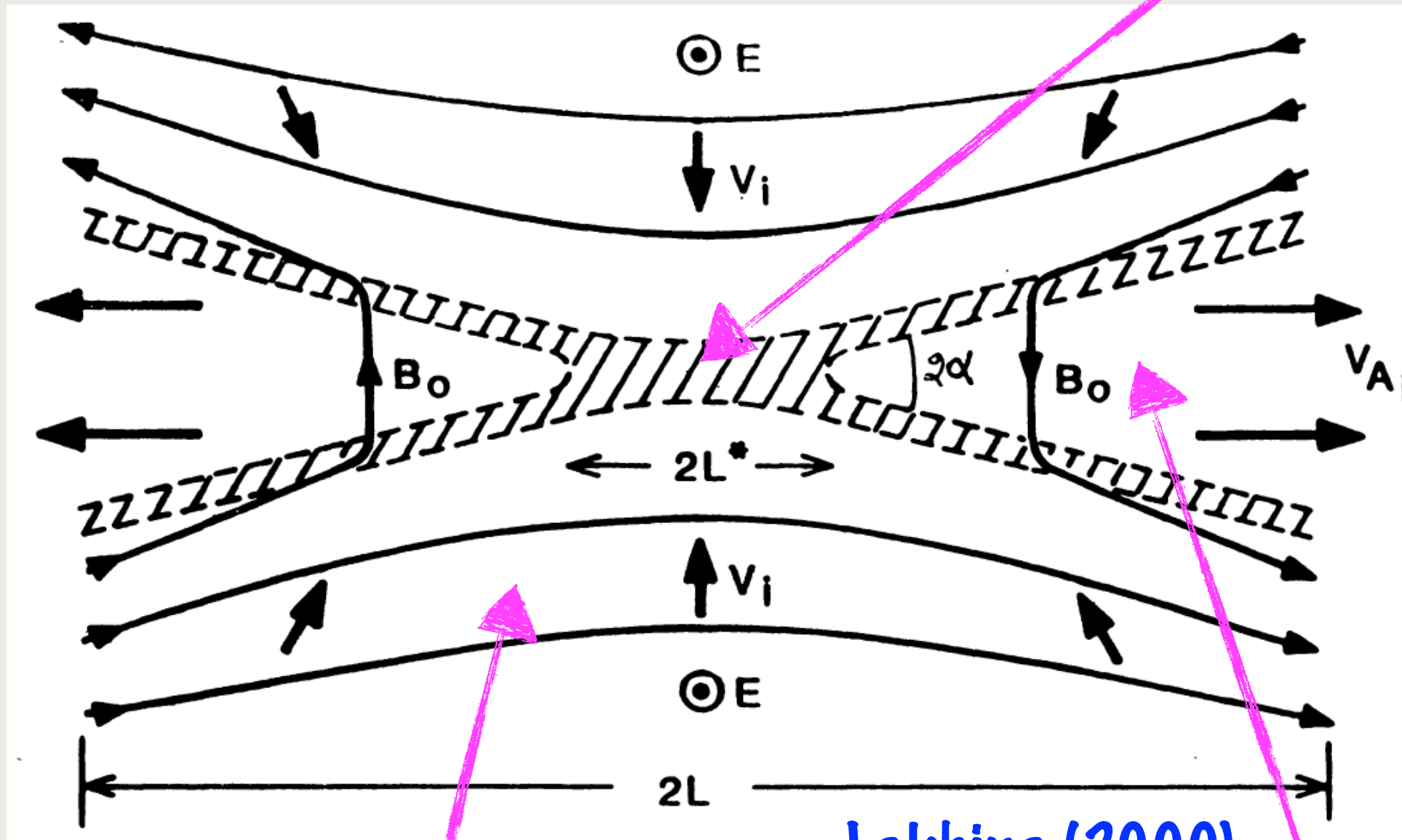
- background magnetization

$$\sigma_0 = B_0^2 / (4\pi n_0 m c^2)$$



MAGNETIC RECONNECTION

magnetic diffusion region (X-point)



$$E \sim \frac{v_{in}}{c} B_0$$

$$v_{in} \sim 0.1 v_{A,0}$$

$$v_{out} \sim v_{A,0}$$

Lakhina (2000)

reconnecting magnetic field
(background, upstream)

reconnection outflow
(downstream)

RECONNECTION OUTFLOW

- Once magnetic field lines are reconnected in the magnetic diffusion region, they are overstretched, magnetic slingshot effect drives outflows $v_y \sim \pm v_{\text{out}}$ (parallel to the background field lines B_x) with $v_{\text{out}} \sim v_{A,0}$ (Alfvén speed of the background plasma).

- These outflows can be relativistic if the background magnetization is relativistic $\sigma_0 \gg 1$, since

$$v_{A,0}/c = \sqrt{\sigma_0/(1 + \sigma_0)}$$

RECONNECTION RATE

- In order for reconnection to be sustained, the outflows need to be balanced by the inflows with velocity $v_{\text{in}} = \beta_{\text{in}}c$ called **the reconnection rate**.
- These inflows induce an electric field $E_z \sim \beta_{\text{in}}B_0$ in the magnetic diffusion region. The electric field is uniform in the stationary case, since $\partial_t B_x = -c \left(\vec{\nabla} \times \vec{E} \right)_x \simeq -c \partial_y E_z \simeq 0$.
- In resistive MHD, the motional field is balanced by the diffusion:

$$\vec{E} \simeq \vec{B} \times \vec{\beta} + \vec{j}/\sigma \simeq \left[\vec{B} \times \vec{v} + \eta(\vec{\nabla} \times \vec{B}) \right] / c$$

$$cE_z \simeq \left[\vec{B} \times \vec{v} + \eta(\vec{\nabla} \times \vec{B}) \right]_z = B_x v_y - \eta \partial_y B_x \simeq 0$$
 this provides the **diffusive reconnection rate** $v_{\text{in}} \sim \eta/\delta$.

LUNDQUIST NUMBER

- Consider a current layer of finite length L
- With the Alfvén speed $v_{A,0}$, this defines a magnetic Reynolds number $R_m = v_{A,0}L/\eta$ also known as **the Lundquist number**
- Conservation of mass and magnetic flux implies
$$v_{\text{in}}L \sim v_{\text{out}}\delta \sim v_{A,0}\delta$$
- Using $v_{\text{in}} \sim \eta/\delta$, one finds $\delta \sim \sqrt{\eta L/v_{A,0}} = L/\sqrt{R_m}$
and hence $v_{\text{in}} \sim \sqrt{\eta v_{A,0}/L} = v_{A,0}/\sqrt{R_m}$

THREE TIME SCALES

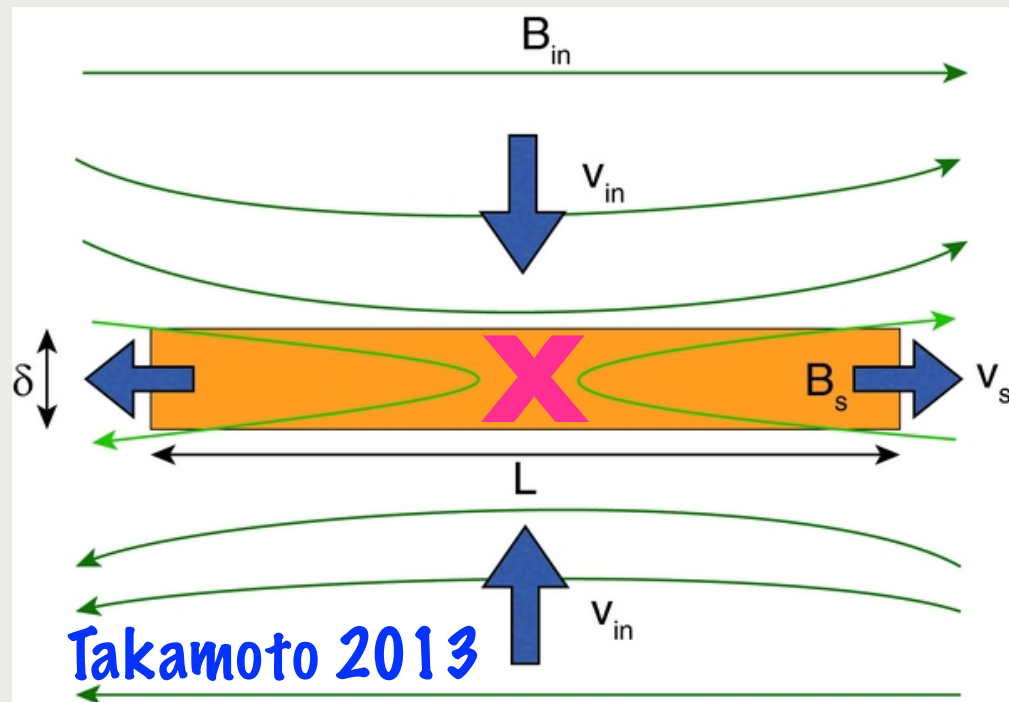
- dynamical (Alfvén): $t_A = L/v_A$
- reconnection: $t_{\text{rec}} = L/v_{\text{in}} \sim \sqrt{R_m} t_A$
- diffusive: $t_\eta = L^2/\eta = R_m t_A$

EXAMPLE: SOLAR FLARES

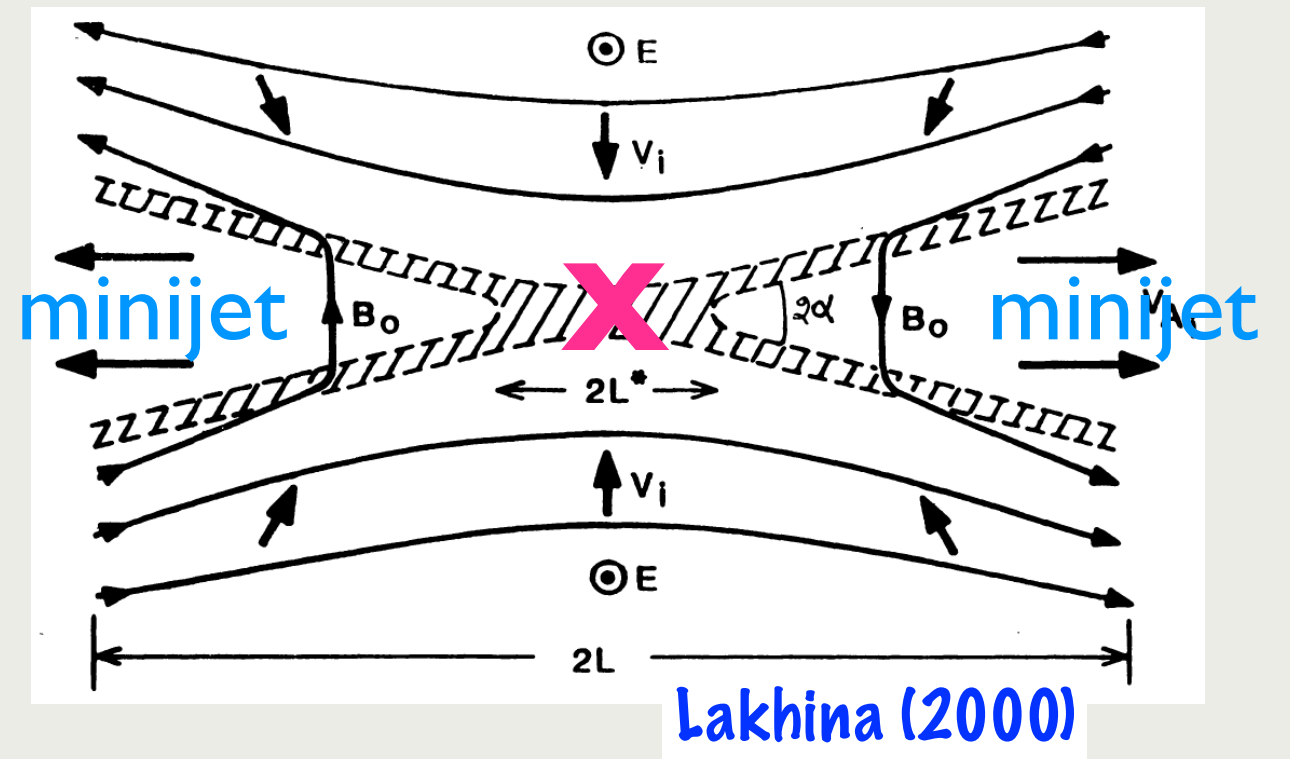
- length scale $L \sim 10^4 \text{ km} = 10^9 \text{ cm}$
- Alfvén speed $v_A \sim 10^{-3} c = 3 \times 10^7 \text{ cm s}^{-1}$
- (Spitzer) magnetic diffusivity $\eta \sim 10^4 \text{ cm}^2 \text{ s}^{-1}$
- Lundquist number $R_m = v_A L / \eta \sim 3 \times 10^{12}$
- diffusive reconnection rate $v_{\text{in}} \sim 2 \text{ cm/s}$
- current layer thickness $\delta \sim 600 \text{ cm}$
- dynamical time scale $t_A \sim 30 \text{ s}$
- reconnection time scale $t_{\text{rec}} \sim 6 \times 10^7 \text{ s} \simeq 2 \text{ yr}$
- diffusive time scale $t_\eta \sim 10^{14} \text{ s} = 3 \text{ Myr}$

RECONNECTION MODELS

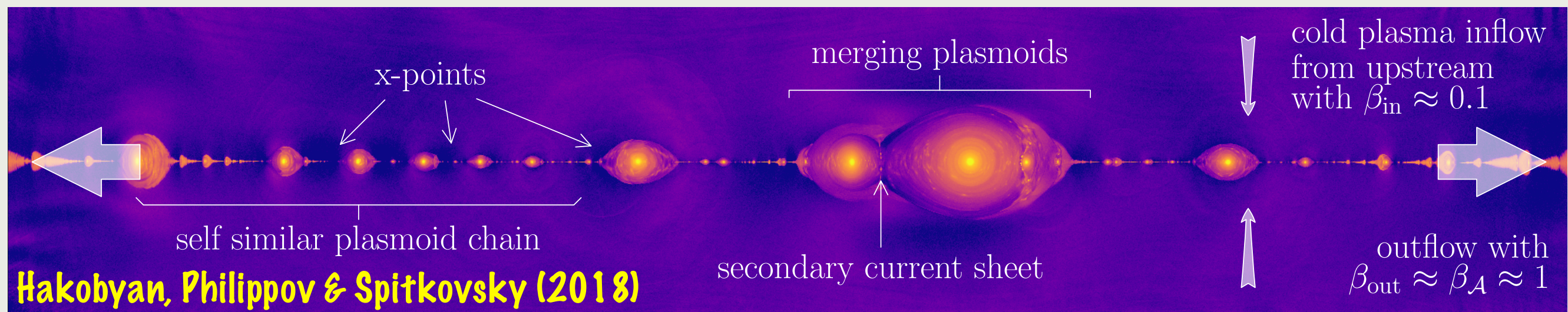
Sweet-Parker



Petschek



plasmoid-dominated



PETSCHEK MODEL

- ion/electron skin depth

$$d = \sqrt{\frac{mc^2}{4\pi e^2 n}}$$

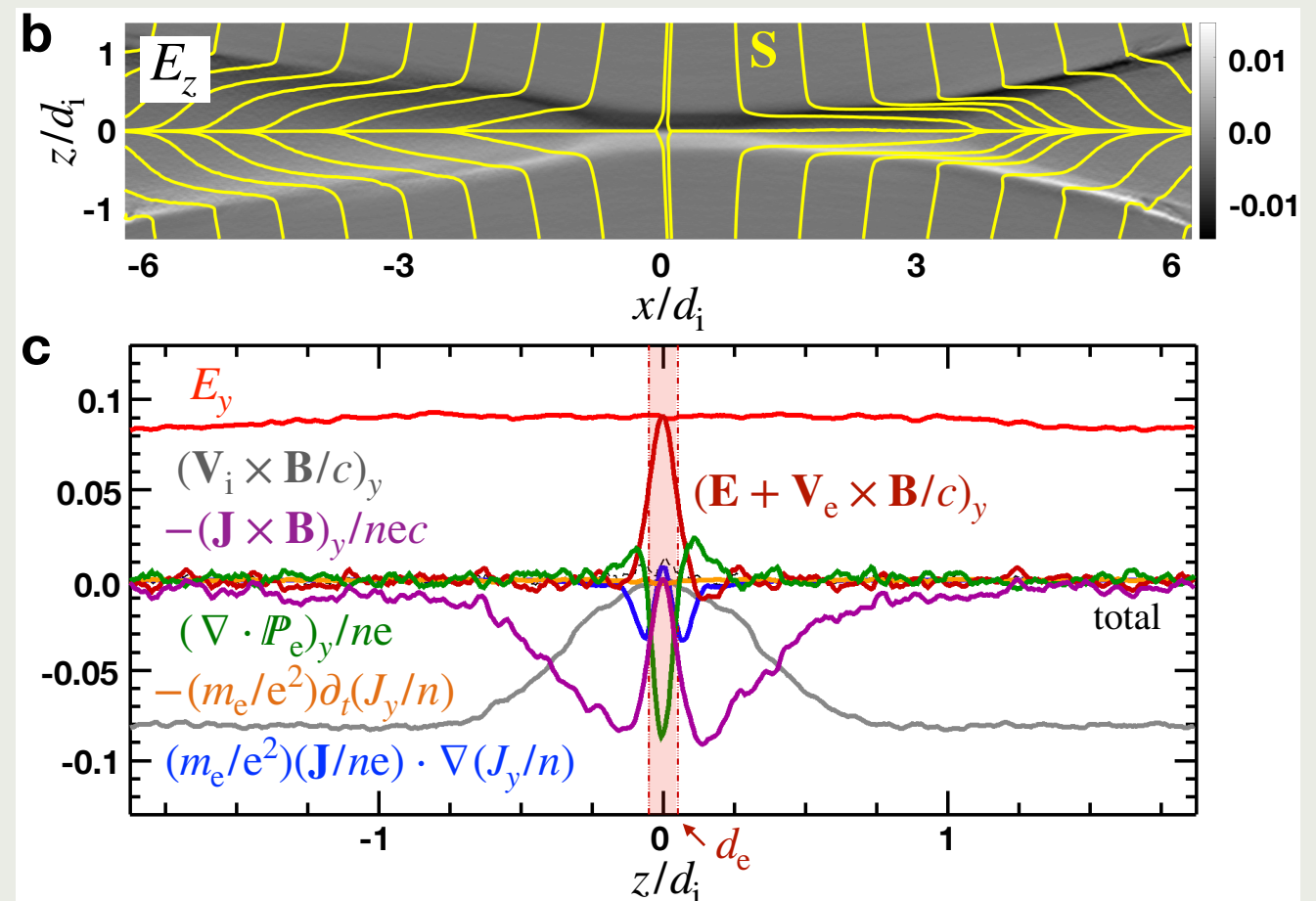
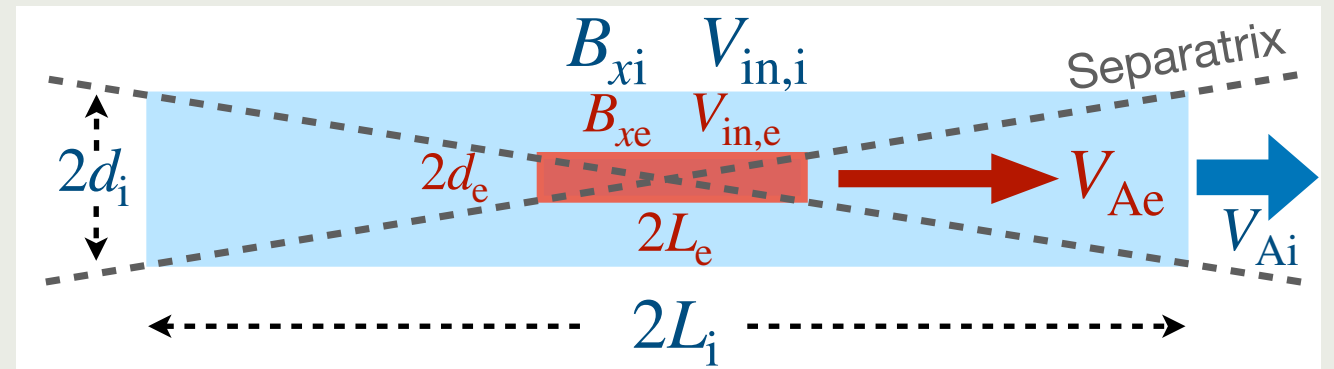
- nested diffusion regions

$$S = \frac{d_i}{L_i} = \frac{d_e}{L_e} \approx \sqrt{\frac{\mu^{1/4} - 1}{3(\mu^{1/4} + 1)}} = 0.49$$

where $\mu = m_i/m_e = 1836$

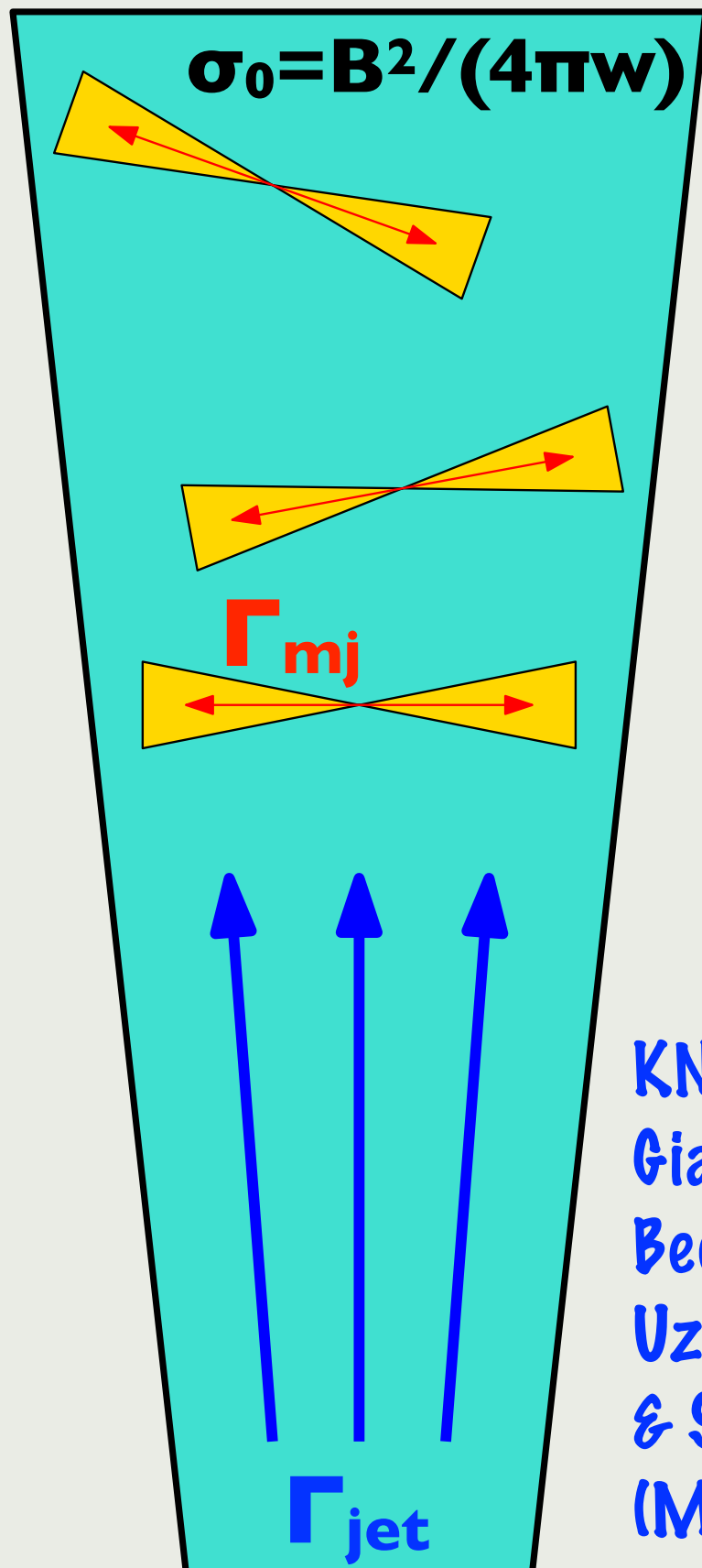
- reconnection rate:

$$\beta \simeq S\sqrt{1 - S^2} \left(\frac{1 - S^2}{1 + S^2} \right)^2 = 0.16$$



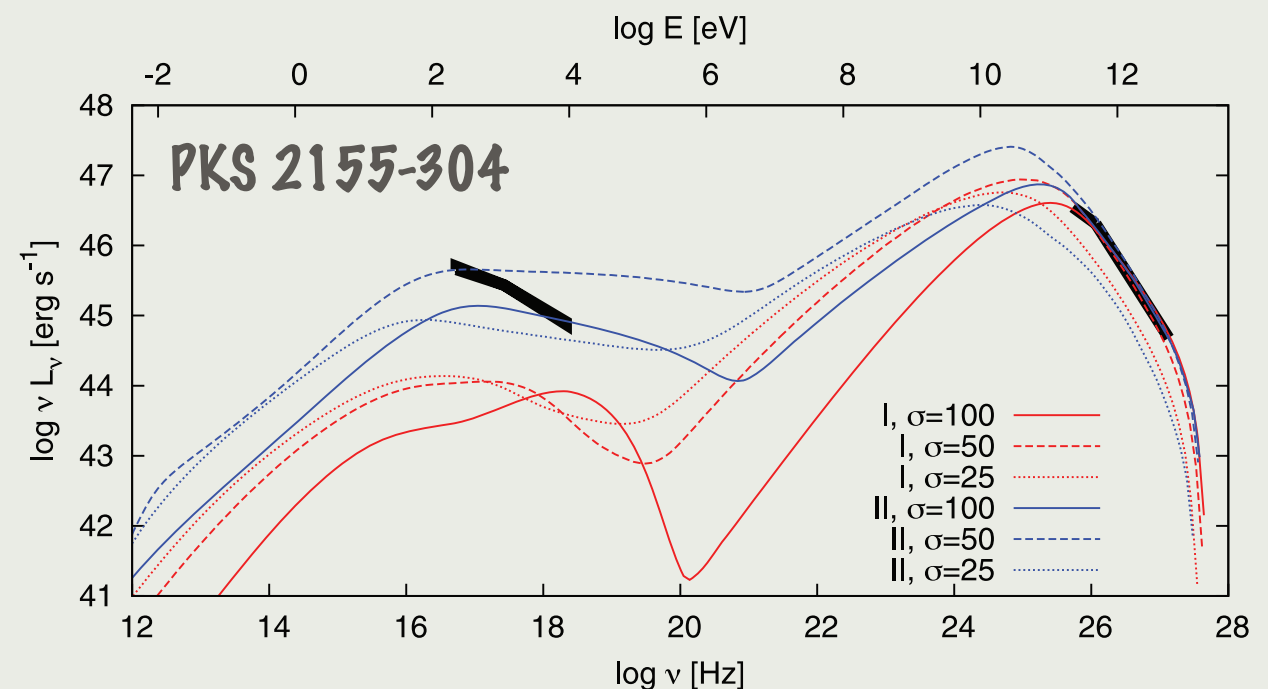
Liu et al. (2022)

MINIJETS MODEL



- reconnection produces localized relativistic outflows (minijets) with Γ_{mj} within a larger relativistic jet
- explains additional relativistic Lorentz boost ($\Gamma_{fl} \sim \Gamma_{jet} \Gamma_{mj}$) and local dissipation
- based on relativistic Petschek reconnection model (Lyubarsky 2005)
- depends on the scaling of minijet Lorentz factor with jet magnetization $\Gamma_{mj} \propto \sigma_0^{1/2}$ in relativistic regime (Giannios, Uzdensky & Begelman 2009)

KN,
Giannios,
Begelman,
Uzdensky
& Sikora
(MNRAS 2011)



TEARING INSTABILITY

The stability of a plane current layer is analyzed in the hydromagnetic approximation, allowing for finite isotropic resistivity. The effect of a small layer curvature is simulated by a gravitational field. In an incompressible fluid, there can be three basic types of “resistive” instability: a long-wave “tearing” mode, corresponding to breakup of the layer along current-flow lines; a short-wave “rippling” mode, due to the flow of current across the resistivity gradients of the layer; and a low- g gravitational interchange mode that grows in spite of finite magnetic shear. The time scale is set by

468

H. P. FURTH, J. KILLEEN, AND M. N. ROSENBLUTH

(1963)

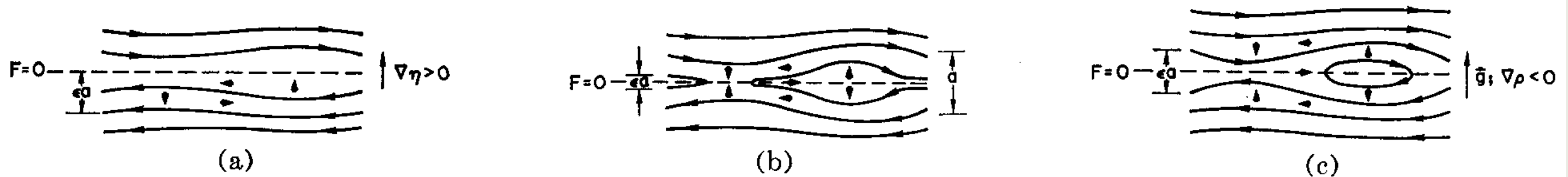


FIG. 2(a) Perturbed fields and velocities—“rippling” mode. Solid arrows indicate fluid velocity. (b) Perturbed fields and velocities—“tearing” mode. (c) Perturbed fields and velocities—gravitational mode.

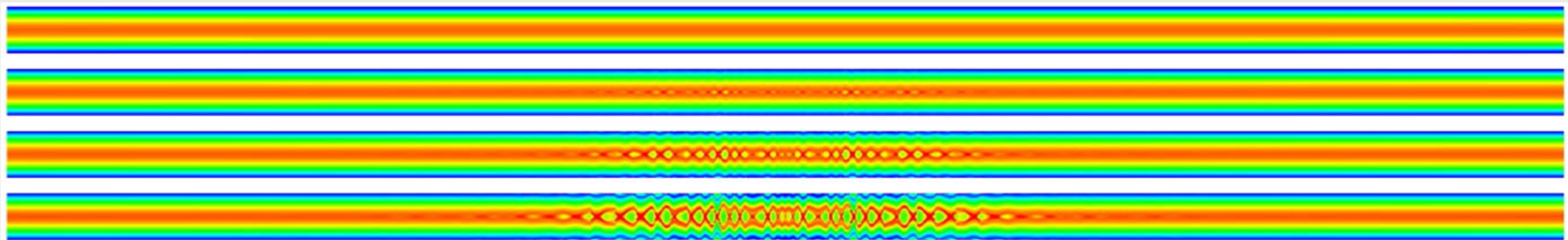


FIG. 1 (color online). Contour plots of the current density showing the time evolution of an SP current sheet for $S = 10^8$. The times shown are, from top to bottom, $t = 0.20\tau_A$, $t = 0.40\tau_A$, $t = 0.45\tau_A$ and $t = 0.50\tau_A$. The domain shown is $-\delta_{SP} \leq x \leq \delta_{SP}$ (inflow direction, vertical), and $-0.12L \leq y \leq 0.12L$ (outflow direction, horizontal), where $\delta_{SP} \approx 10^{-4}$ is the SP layer width and $L = 1$ is the (half-)length of the current sheet (see text; only the central half of the simulation box is shown).

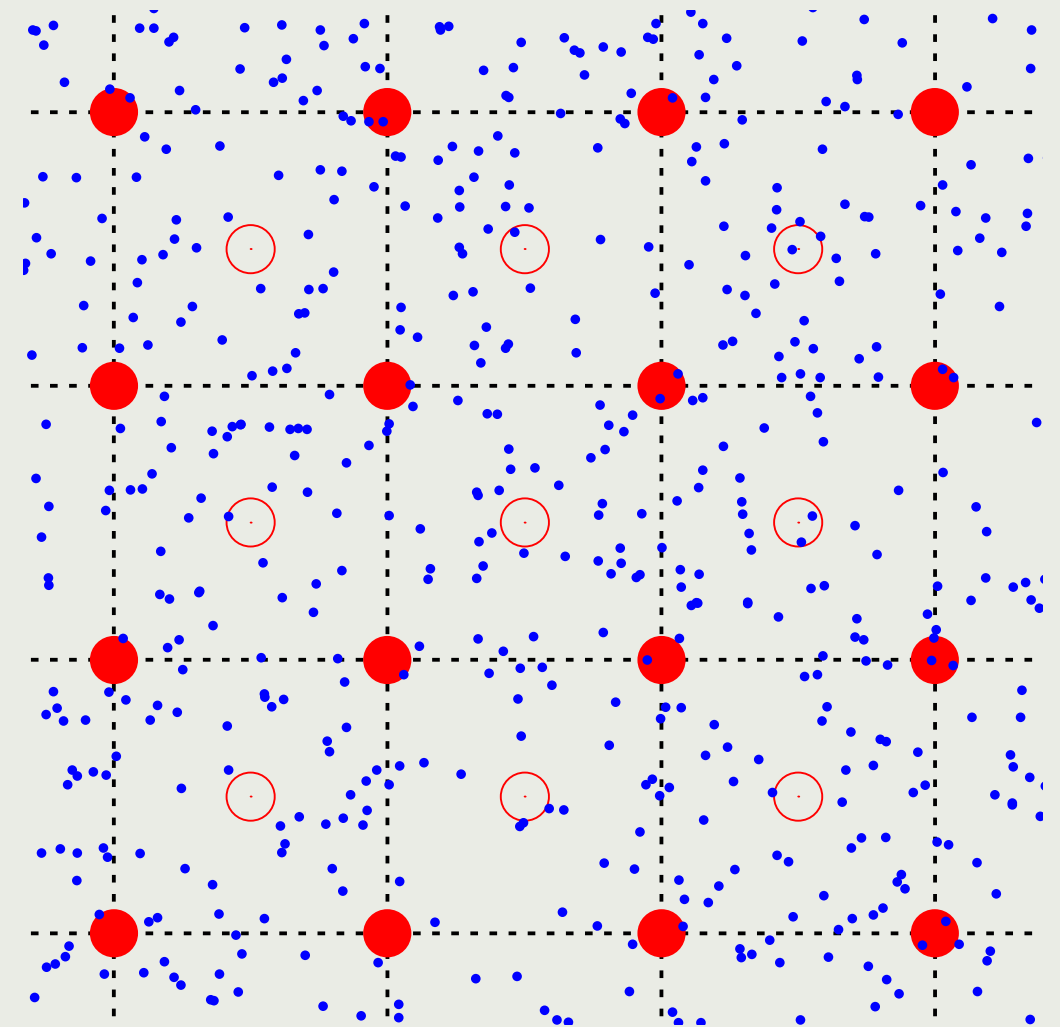
Samtaney et al. (2009)

KINETIC SIMULATIONS

PARTICLE-IN-CELL ALGORITHM

KINETIC NUMERICAL SIMULATIONS OF PLASMAS

- staggered grid of E,B fields
- many discrete charged particles per cell
- particles advanced under Lorentz force
- charge and current density deposited on the grid
- E,B fields advanced according to Maxwell's equations

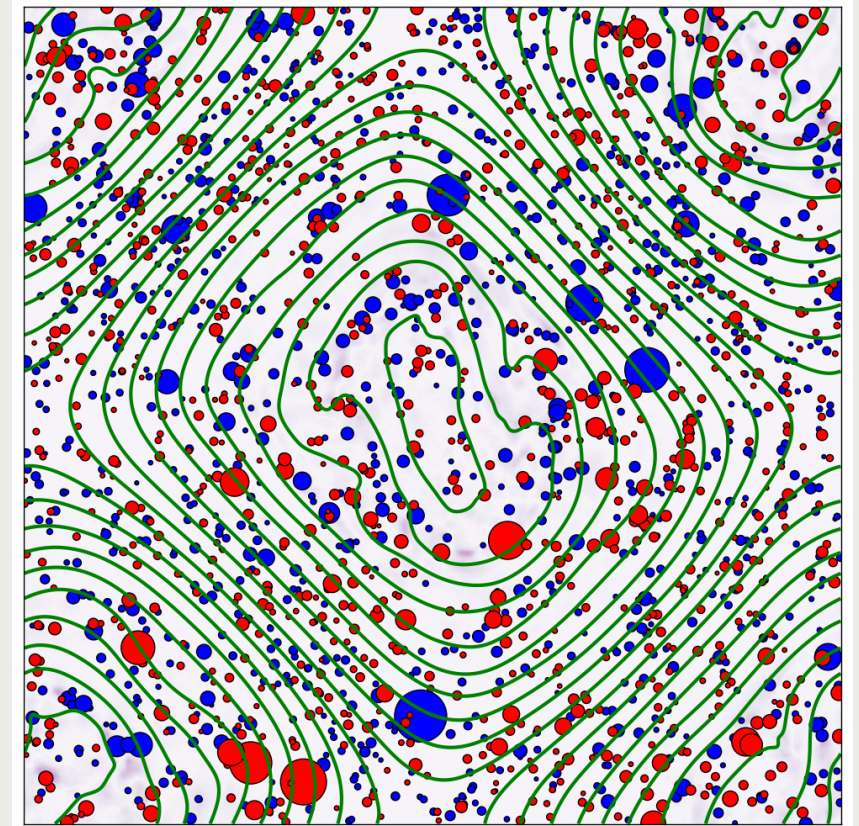
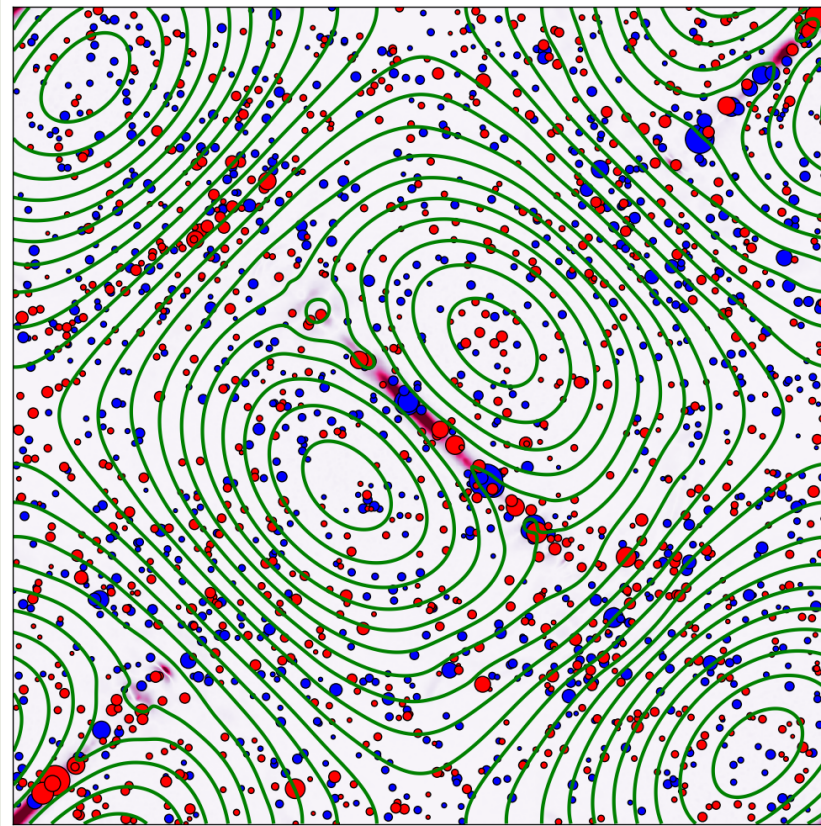
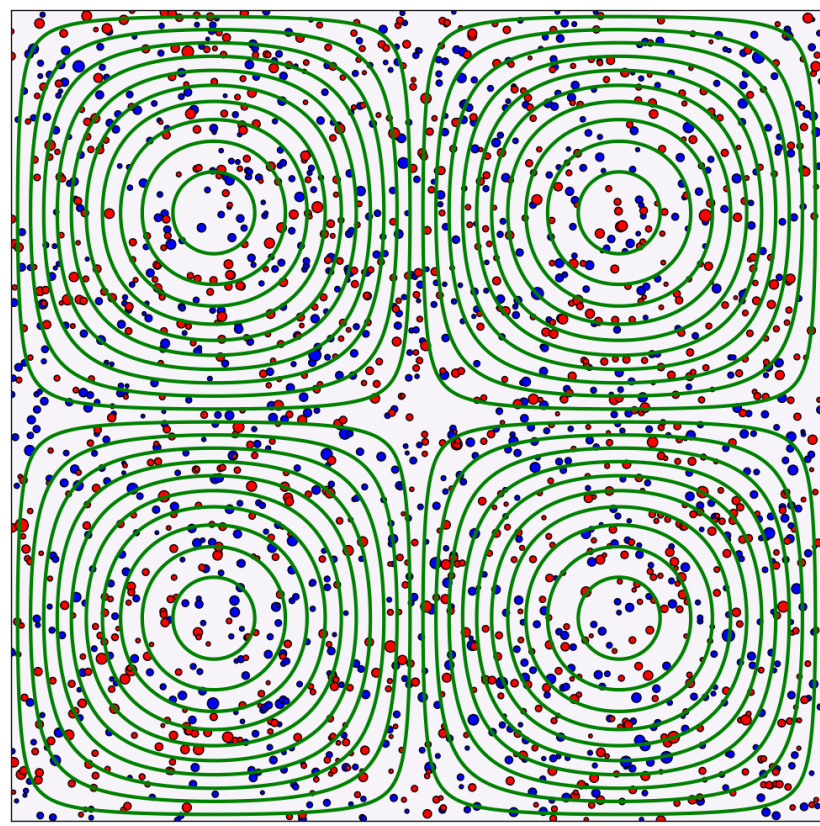


ZELTRON code

Cerutti et al. (2013)

<http://benoit.cerutti.free.fr/Zeltron/>

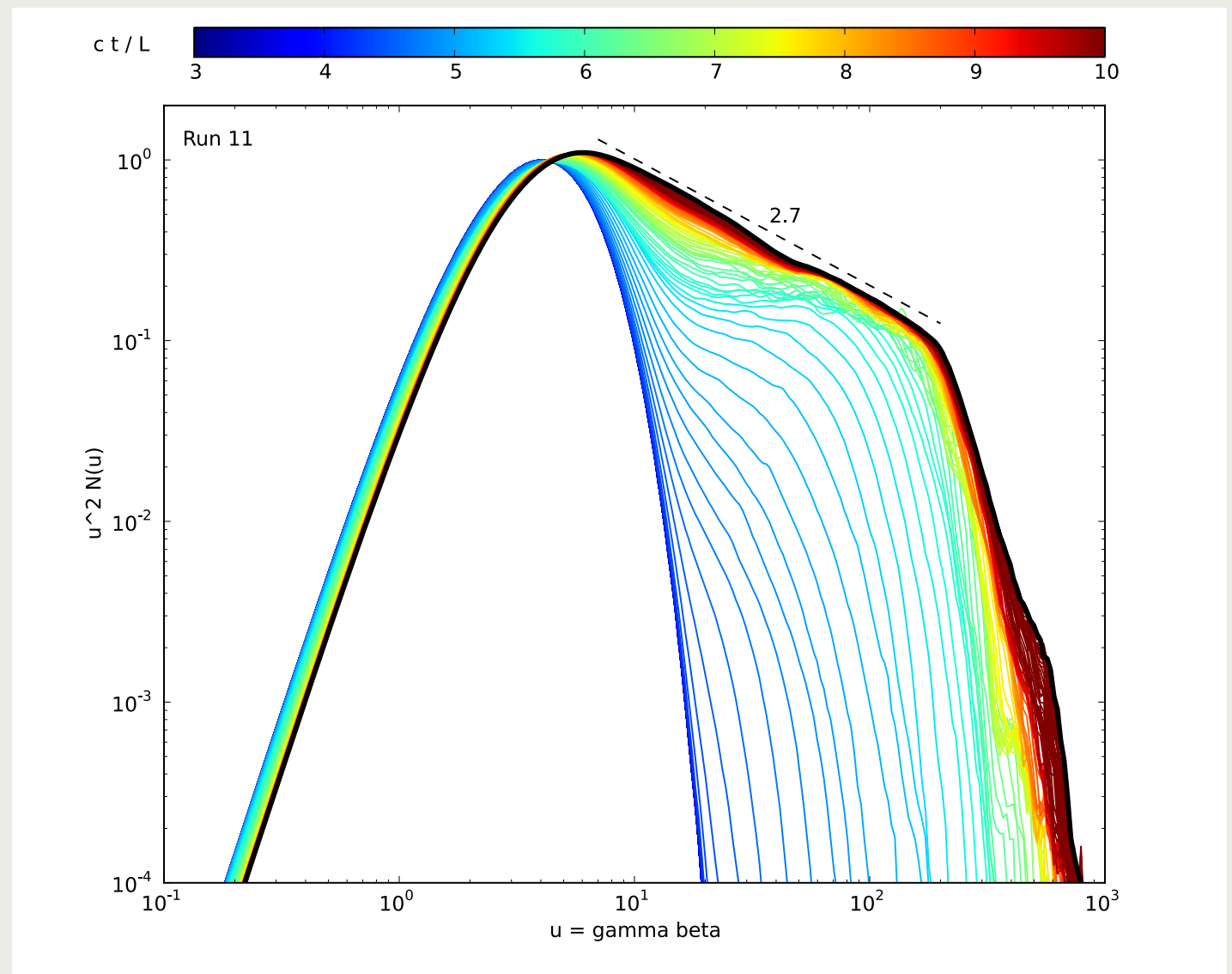
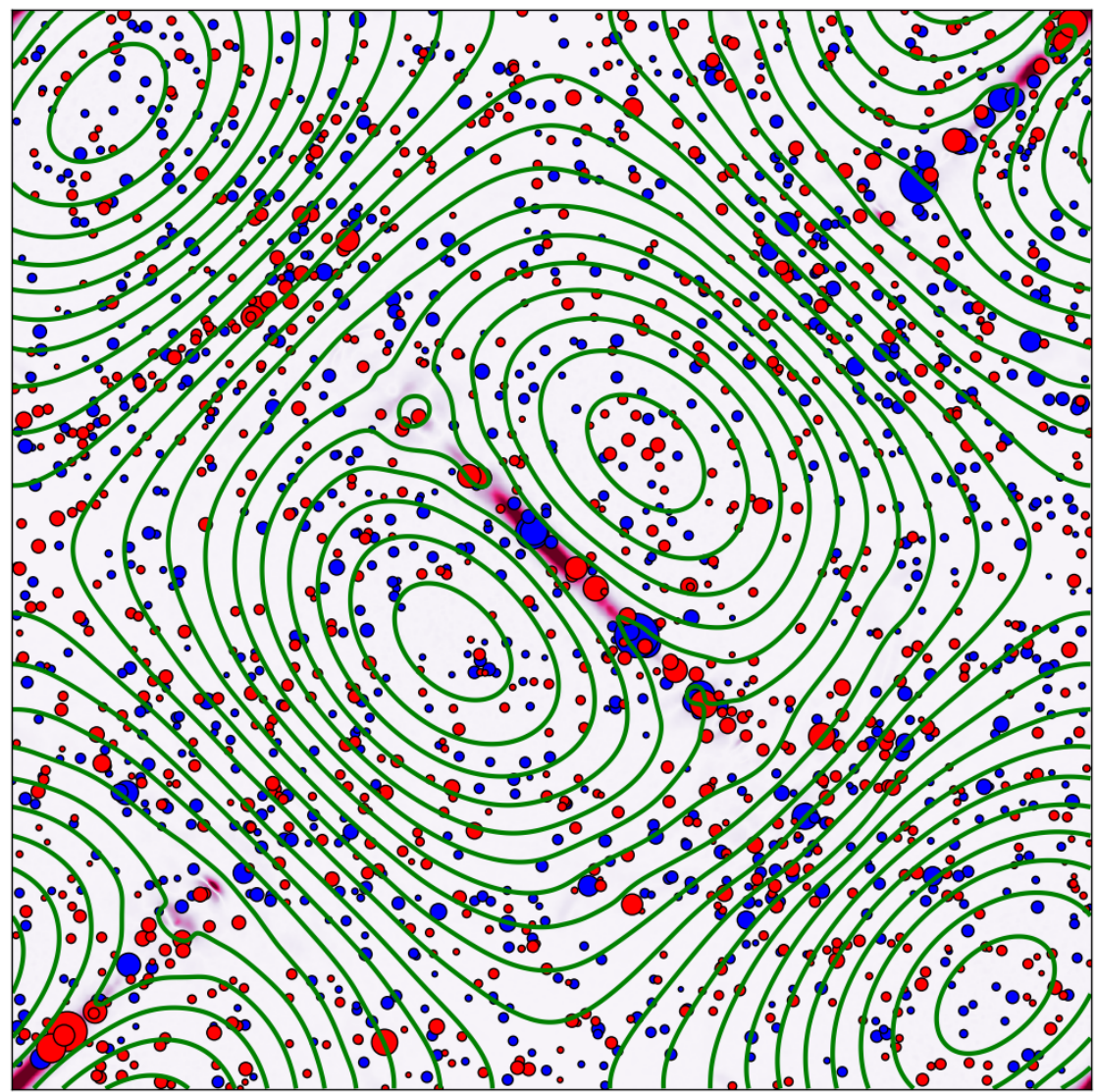
PARTICLE-IN-CELL NUMERICAL SIMULATIONS



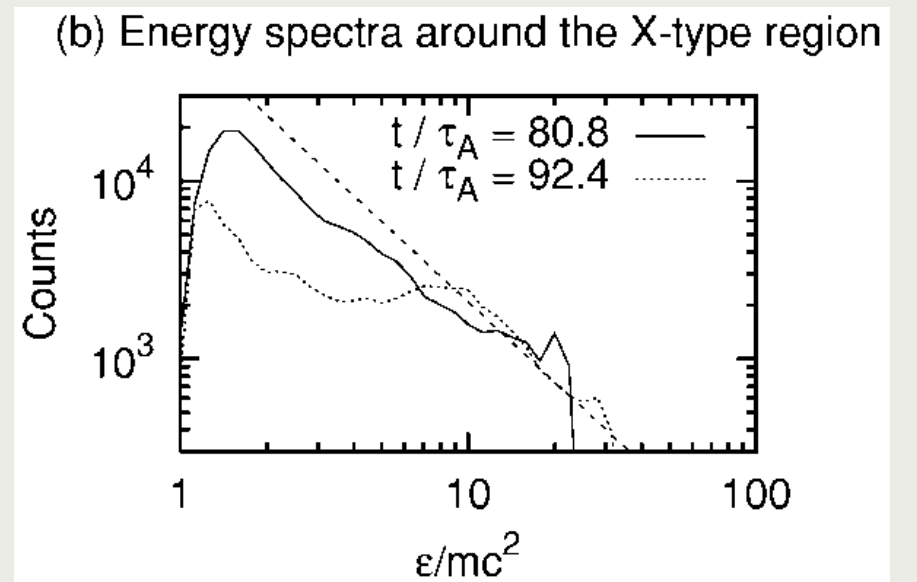
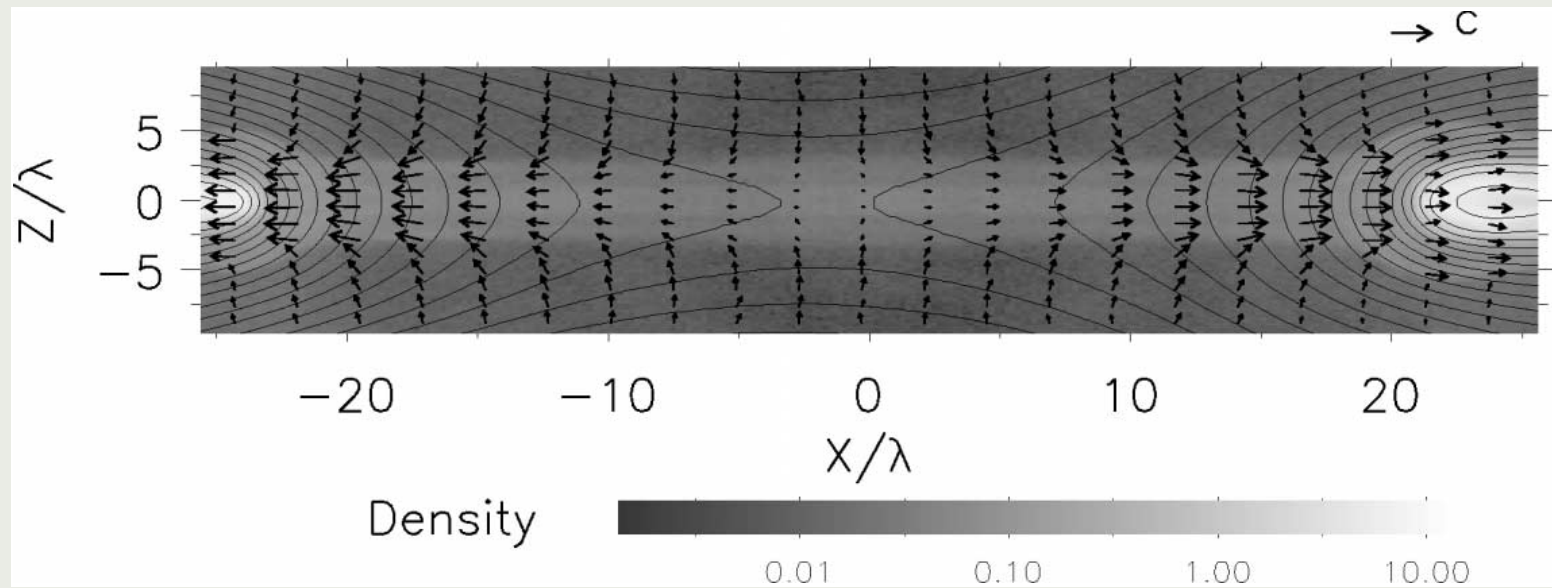
publicly available PIC code Zeltron
created by Benoît Cerutti
<http://benoit.cerutti.free.fr/Zeltron/>

this is a 2D PIC simulation
with 4096^2 cells
and 2 billion particles
computed on 256 CPUs
85k time steps in 14 days

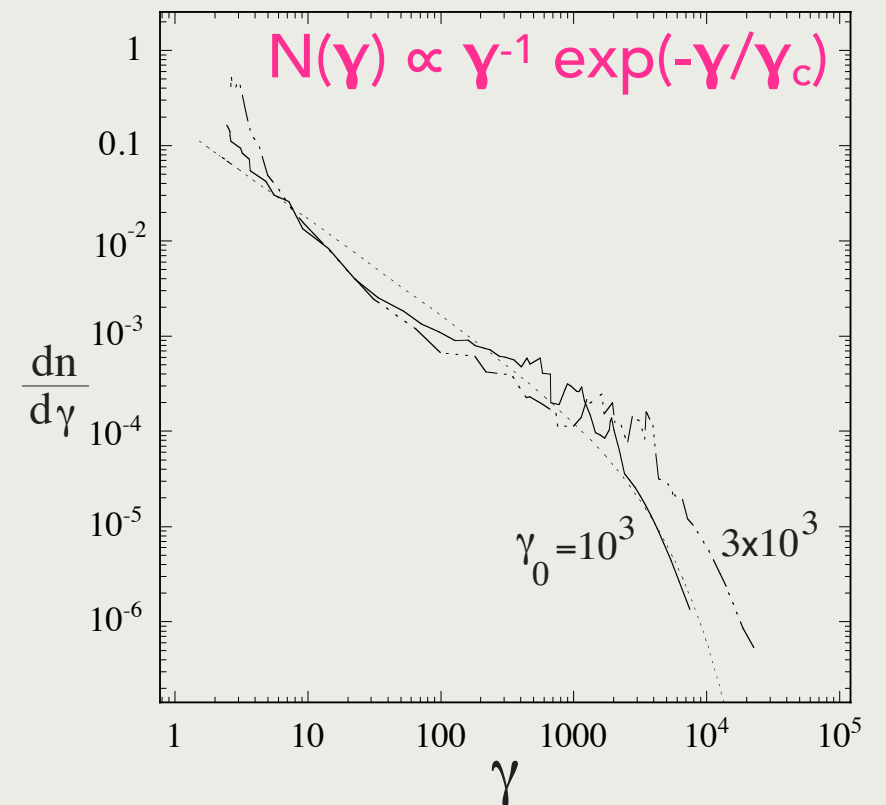
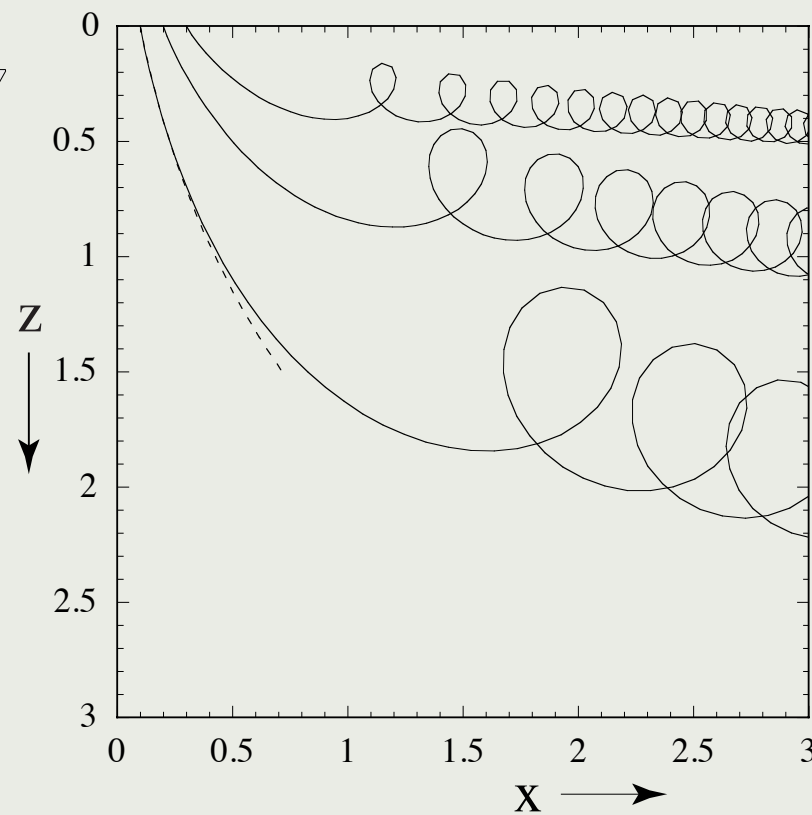
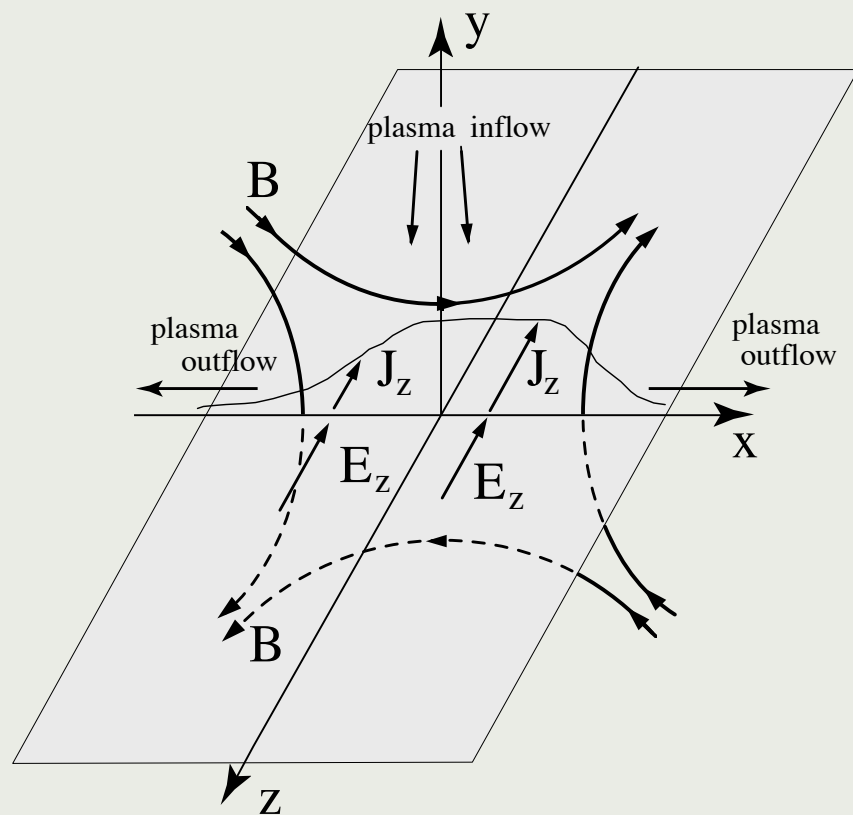
PARTICLE ACCELERATION WITH PIC



PARTICLE ACCELERATION IN RELATIVISTIC RECONNECTION



particle-in-cell simulations: Zenitani & Hoshino (2001)



iterative integration of test particles: Larrabee, Lovelace & Romanova (2003)

PARTICLE ACCELERATION IN RELATIVISTIC PAIR-PLASMA RECONNECTION

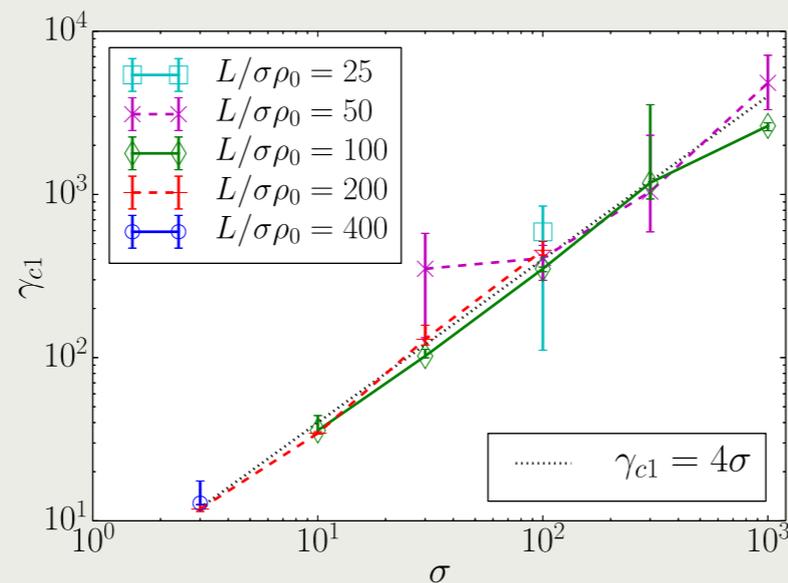
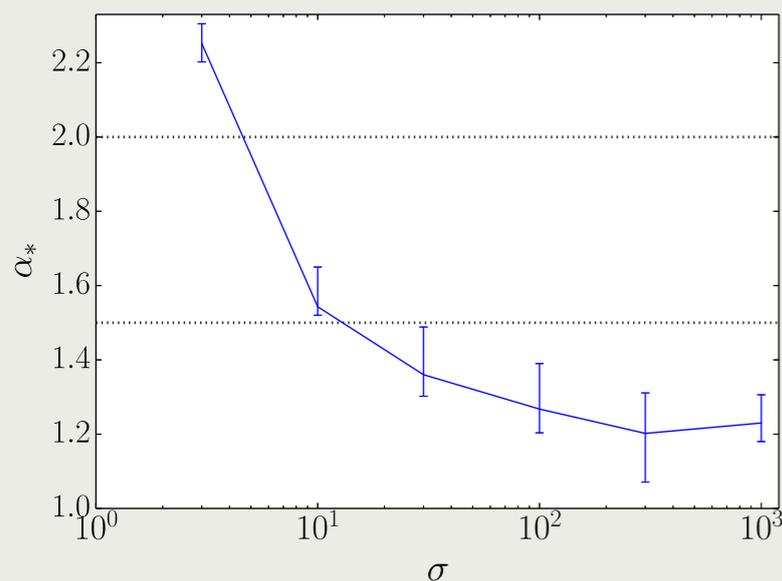
- reconnection produces power-law distributions that are hardening with increasing sigma

$$N(\gamma) \propto \gamma^{-p}, p \rightarrow 1 \text{ for } \sigma \gg 1$$

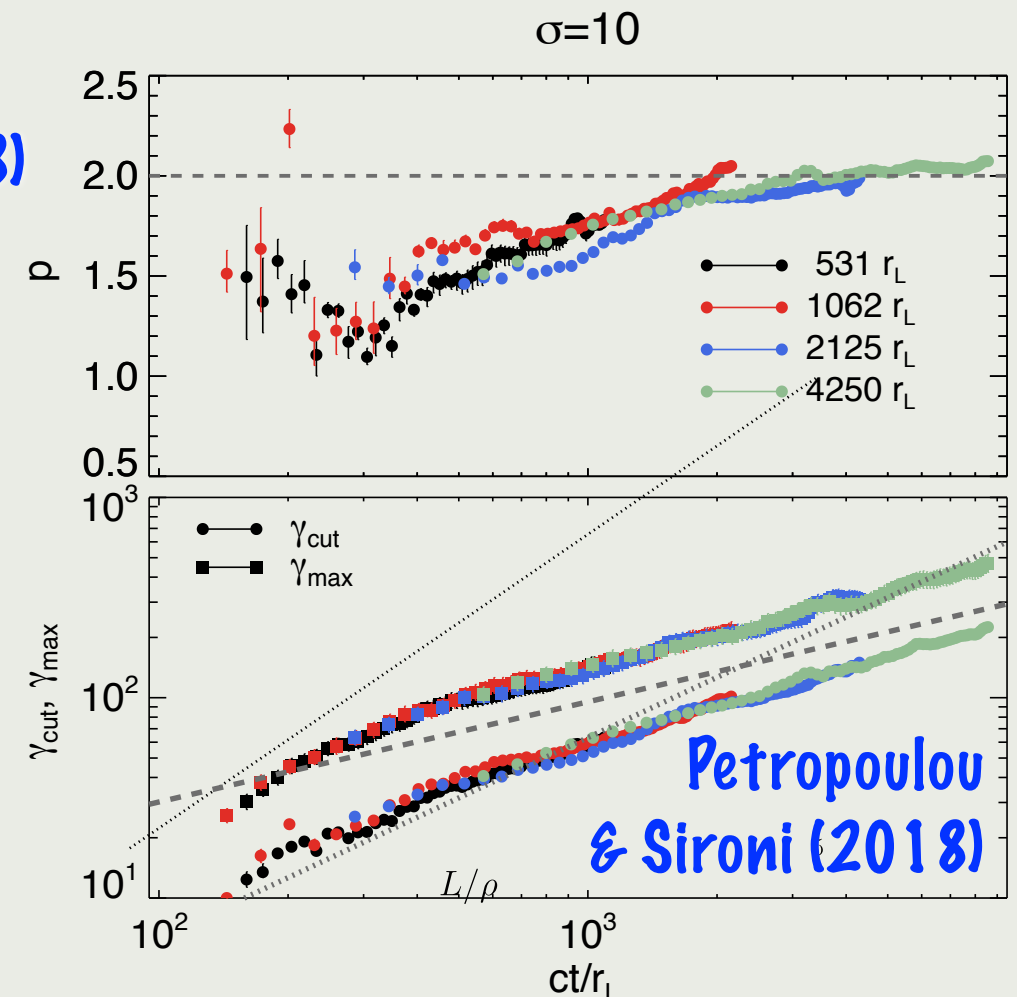
(Sironi & Spitkovsky 2014, Guo et al. 2014, Werner et al. 2016)

- high-energy cut-off is exponential with $\gamma_{\max} \propto \sigma$

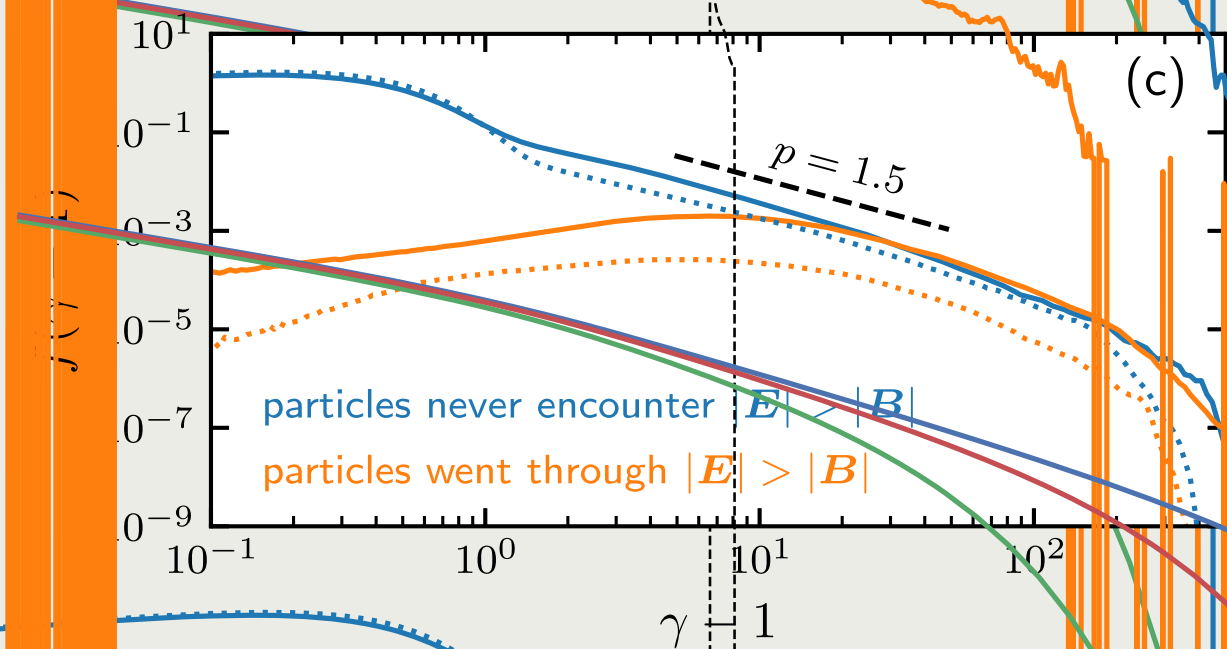
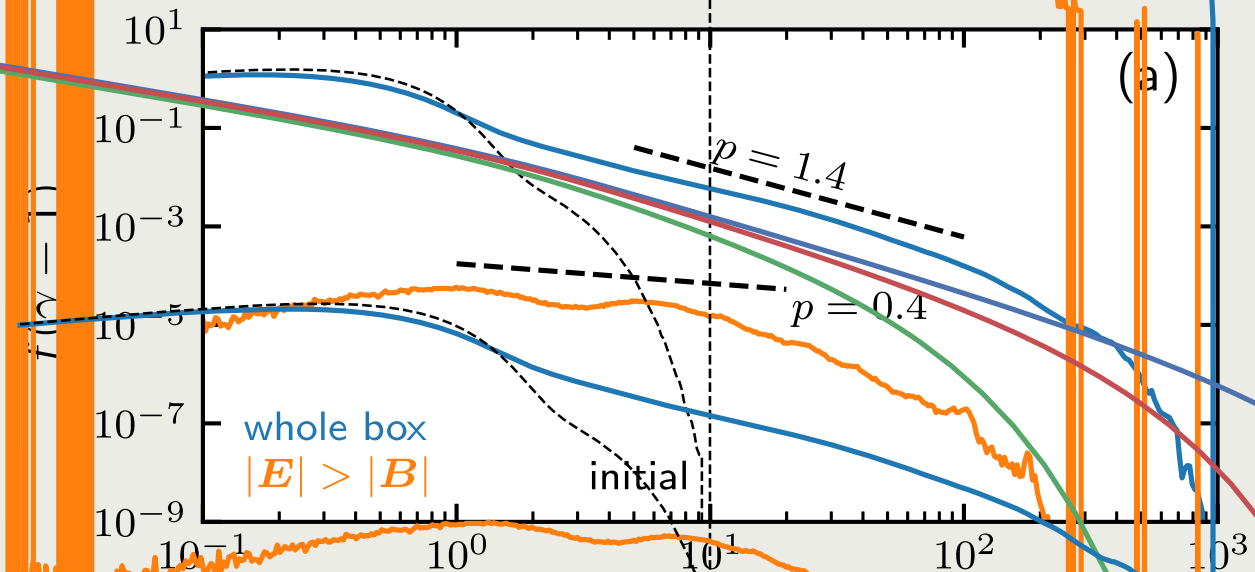
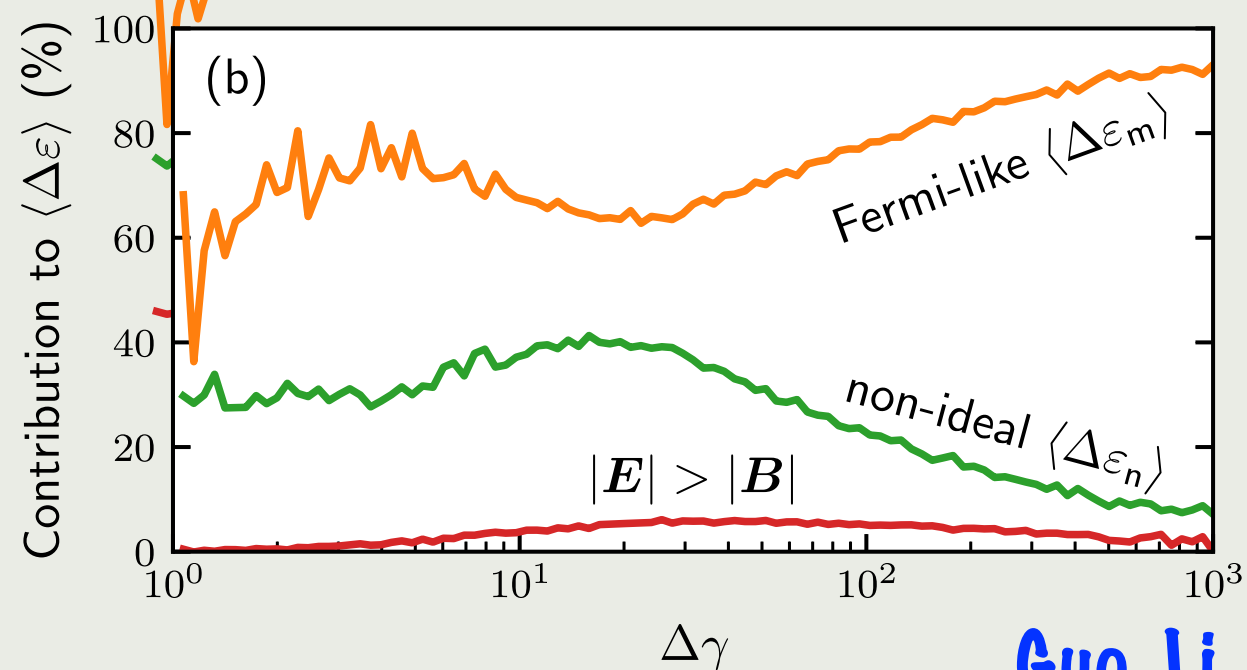
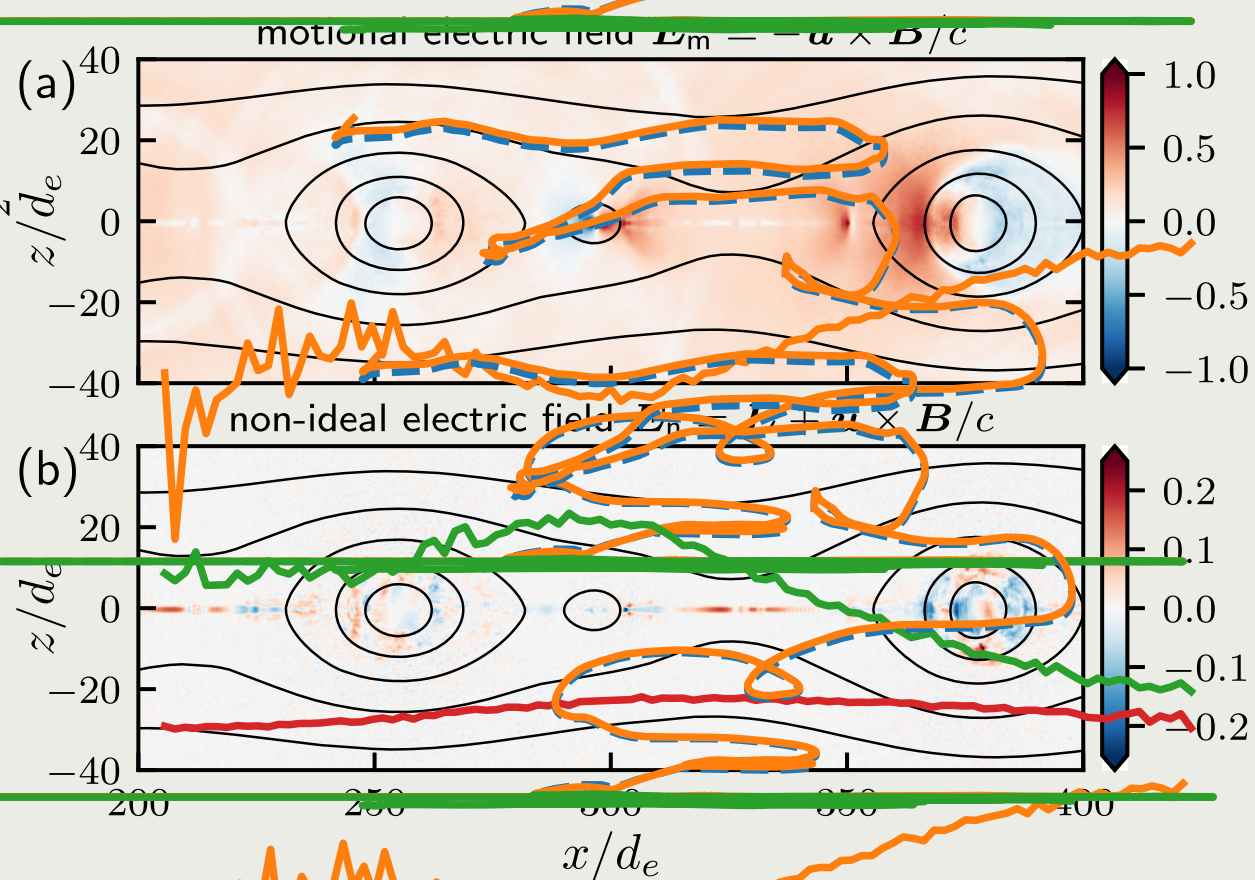
- $p \rightarrow 2$ in very large plasmoids (Petropoulou & Sironi 2018)



Werner, Uzdensky, Cerutti, KN & Begelman (2016)



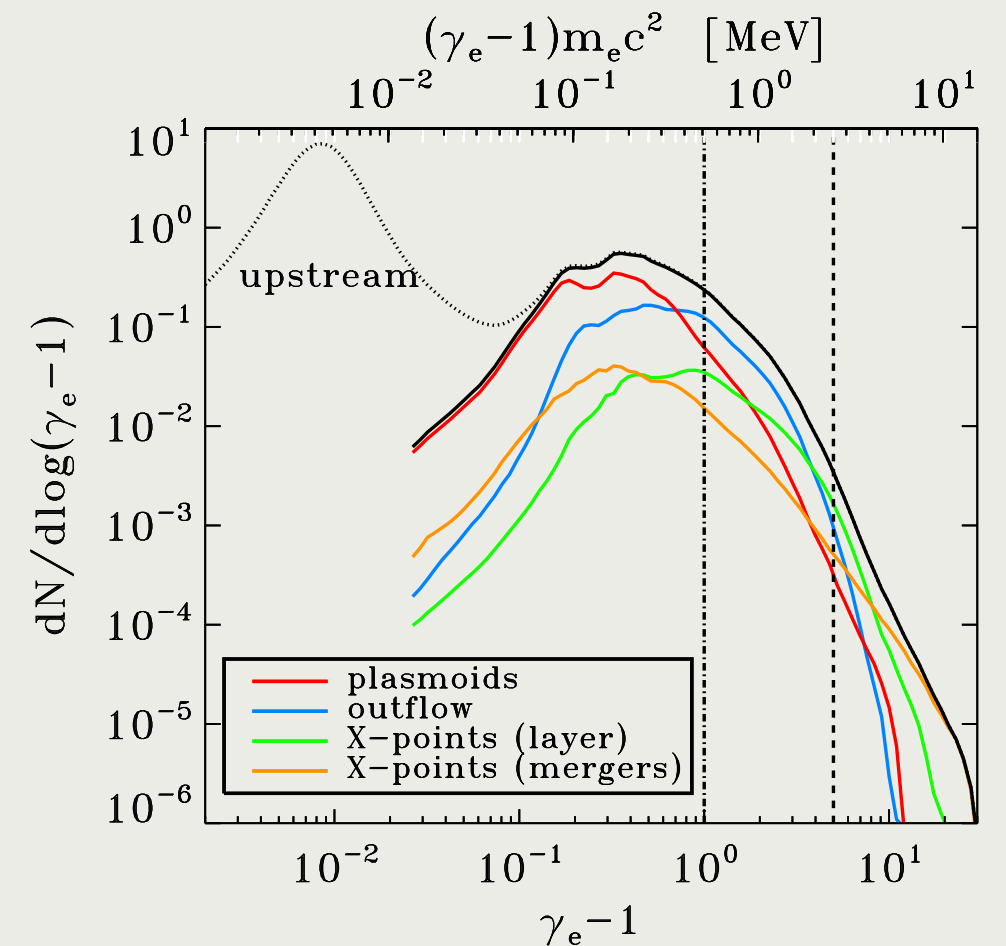
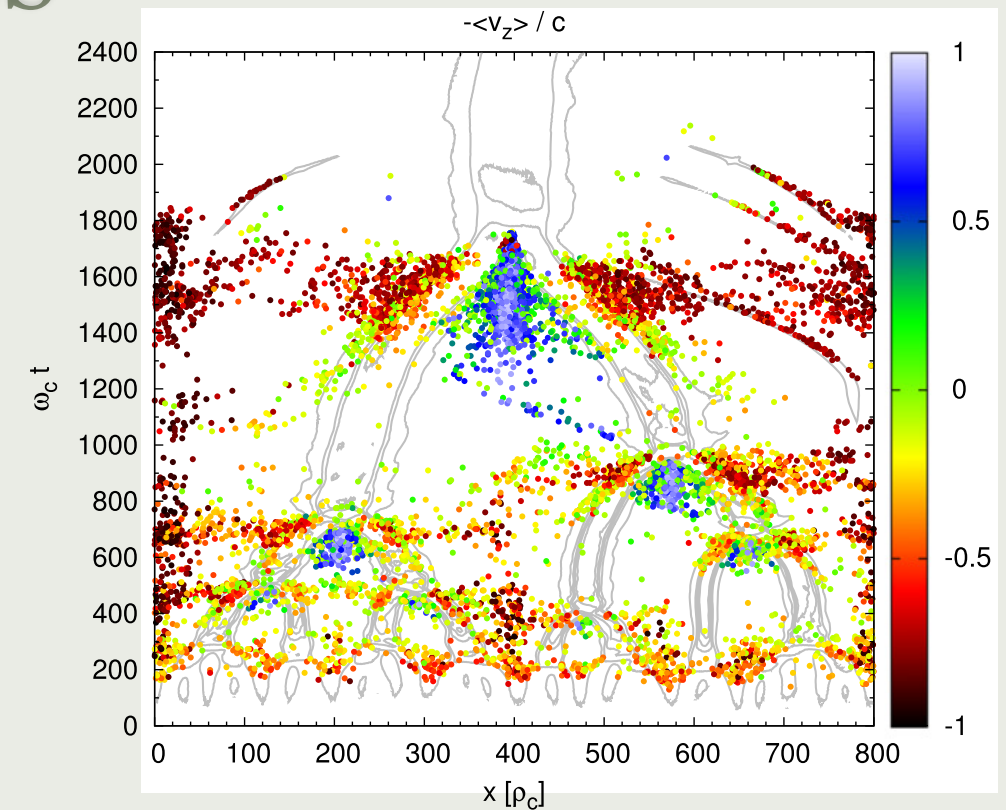
IDEAL VS. NON-IDEAL ELECTRIC FIELD



PARTICLE ACCELERATION SITES

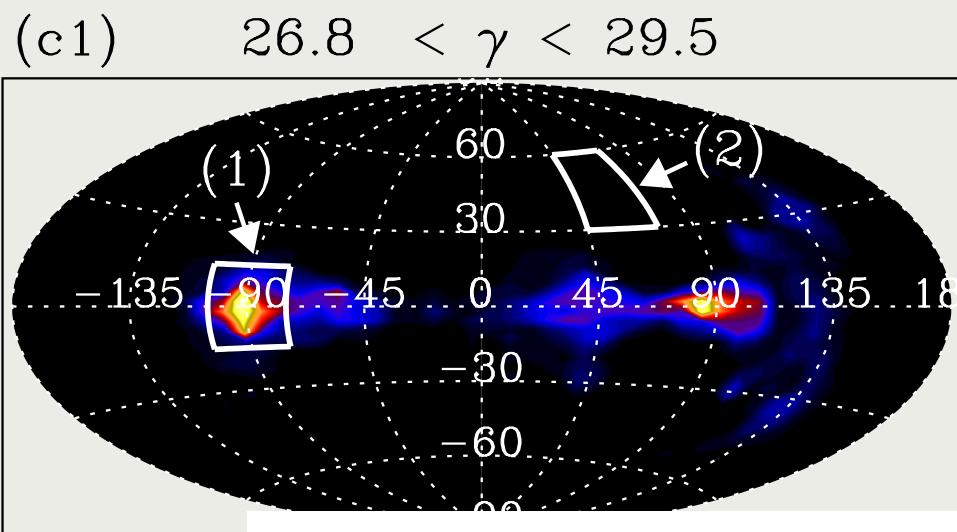
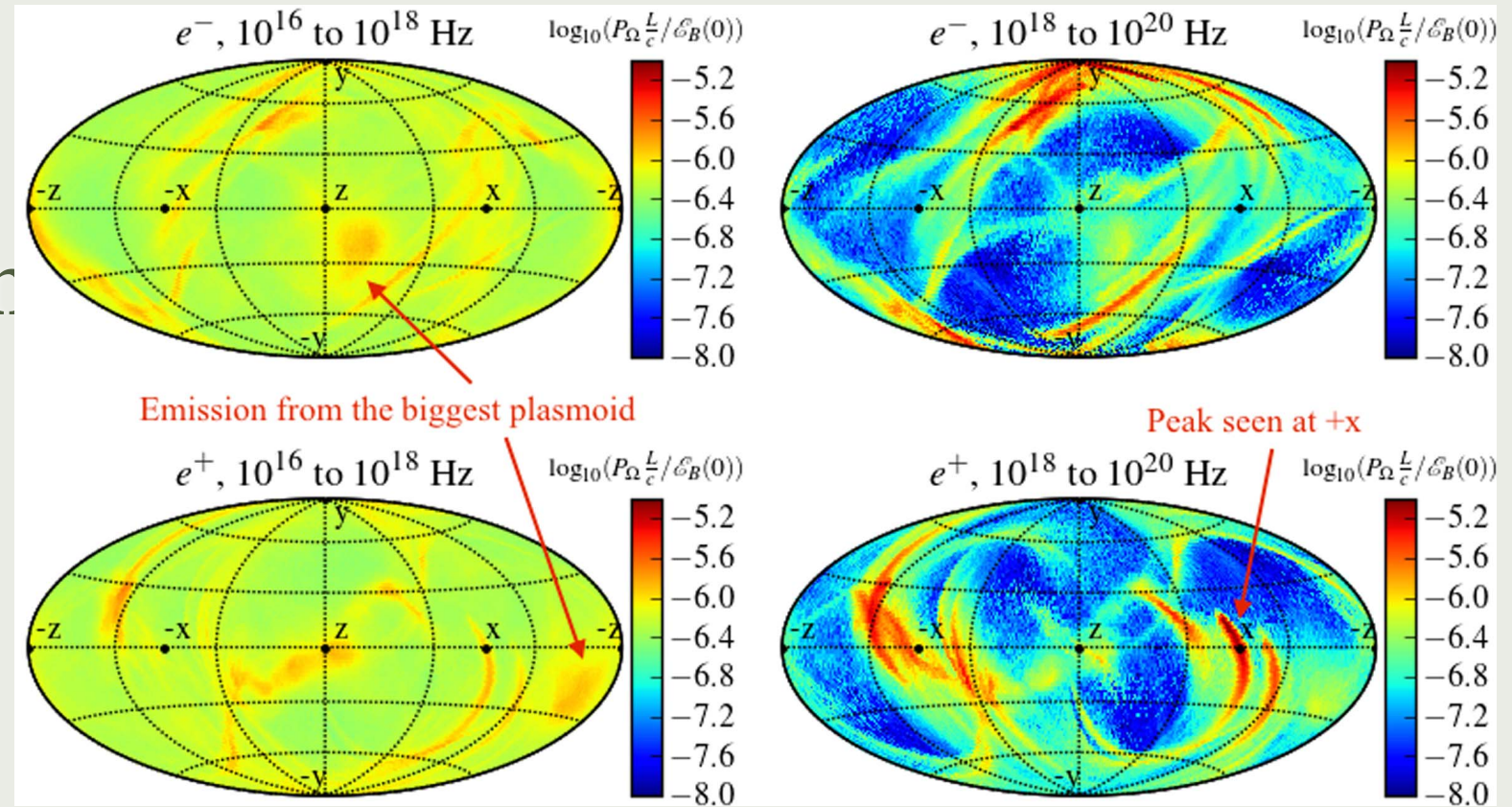
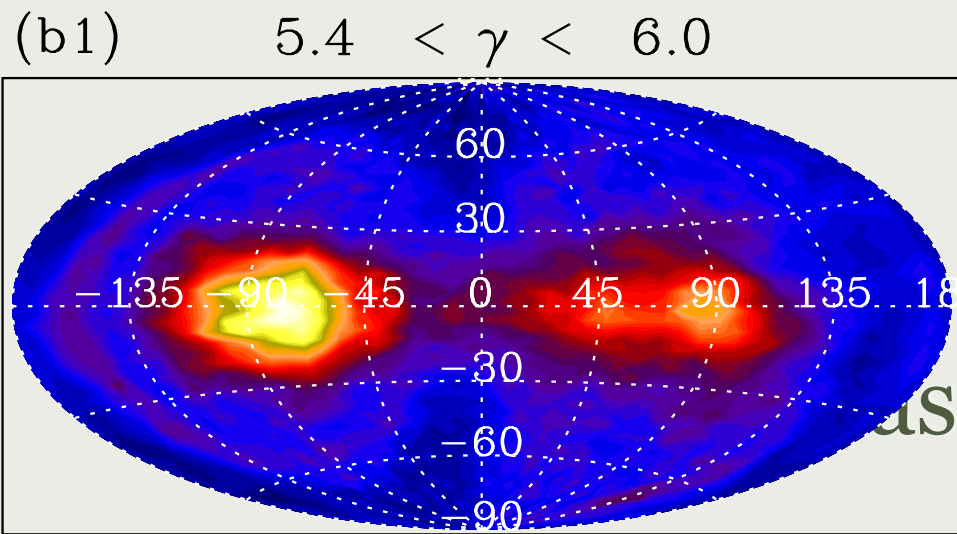
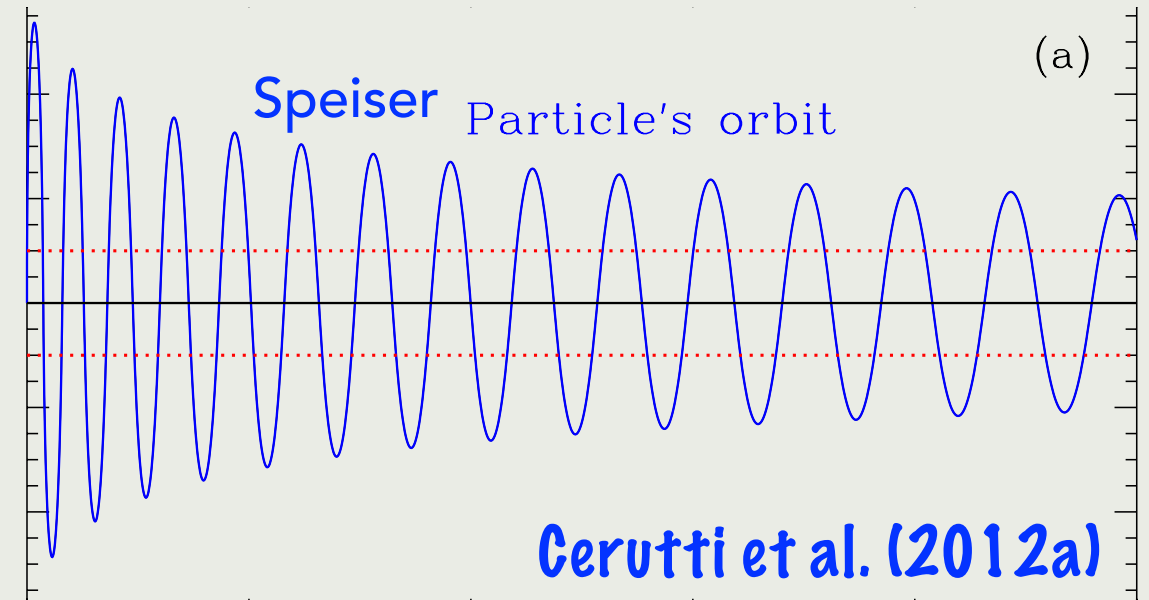
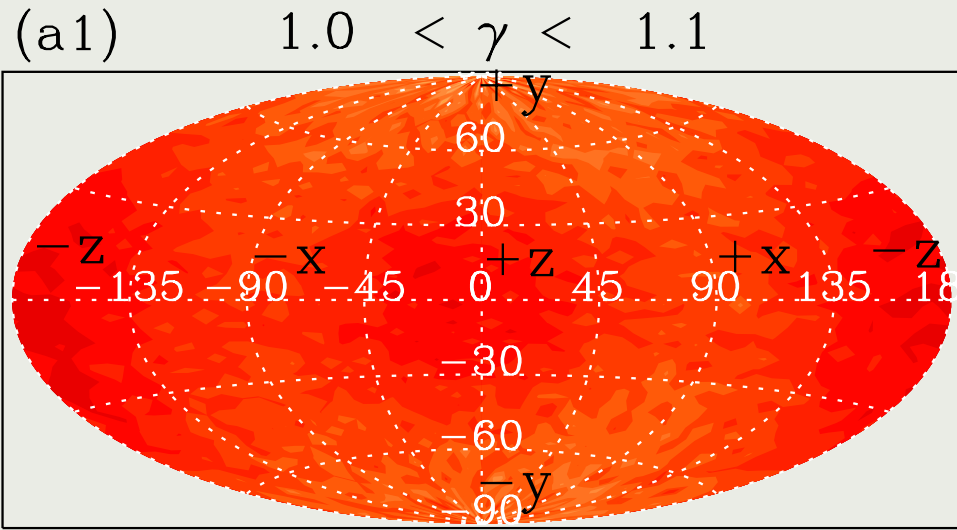
KN et al. (2015)

- **magnetic diffusion regions (X-points):**
non-ideal E-fields (Zenitani & Hoshino 2001)
most energetic particles pass through them (Sironi & Spitkovsky 2014)
short interaction times (Guo et al. 2019)
- **reconnection outflows (minijets):**
Speiser orbits
exceeding radiation reaction (Kirk 2004)
low particle density
- **plasmoids:**
converging “magnetic mirror” (Drake et al. 2006)
contracting cores (Petropoulou & Sironi 2018)
particle traps, high particle density
limited by radiation reaction
- **plasmoid mergers:**
secondary reconnection layers
production of rapid and luminous flares (KN et al. 2015, Ortuño-Macías & KN 2020)



Sironi & Beloborodov (2020)

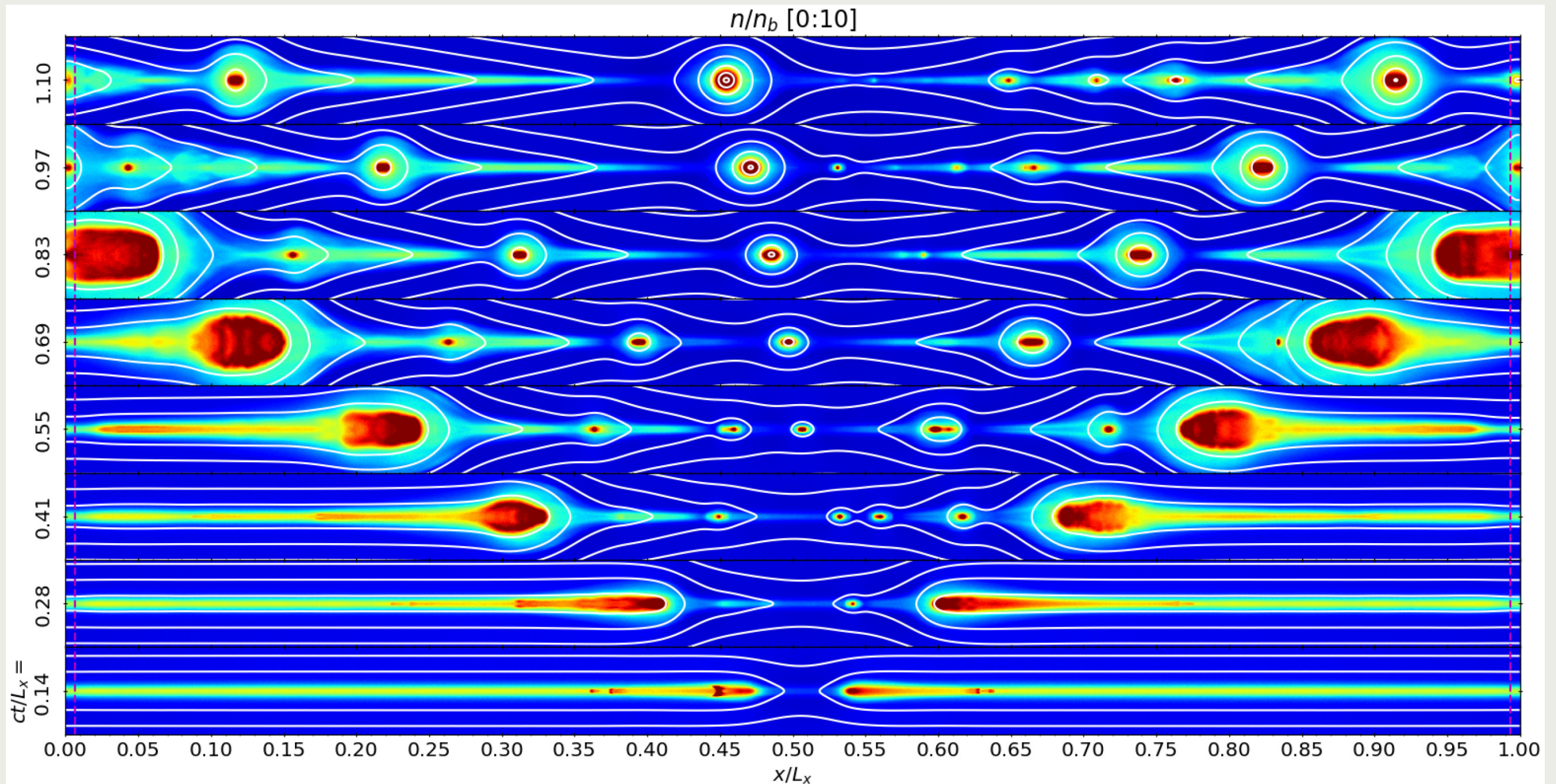
KINETIC BEAMING: ENERGY-DEPENDENT PARTICLE ANISOTROPY



Cerutti et al. (2012b)

Yuan et al. (2016)

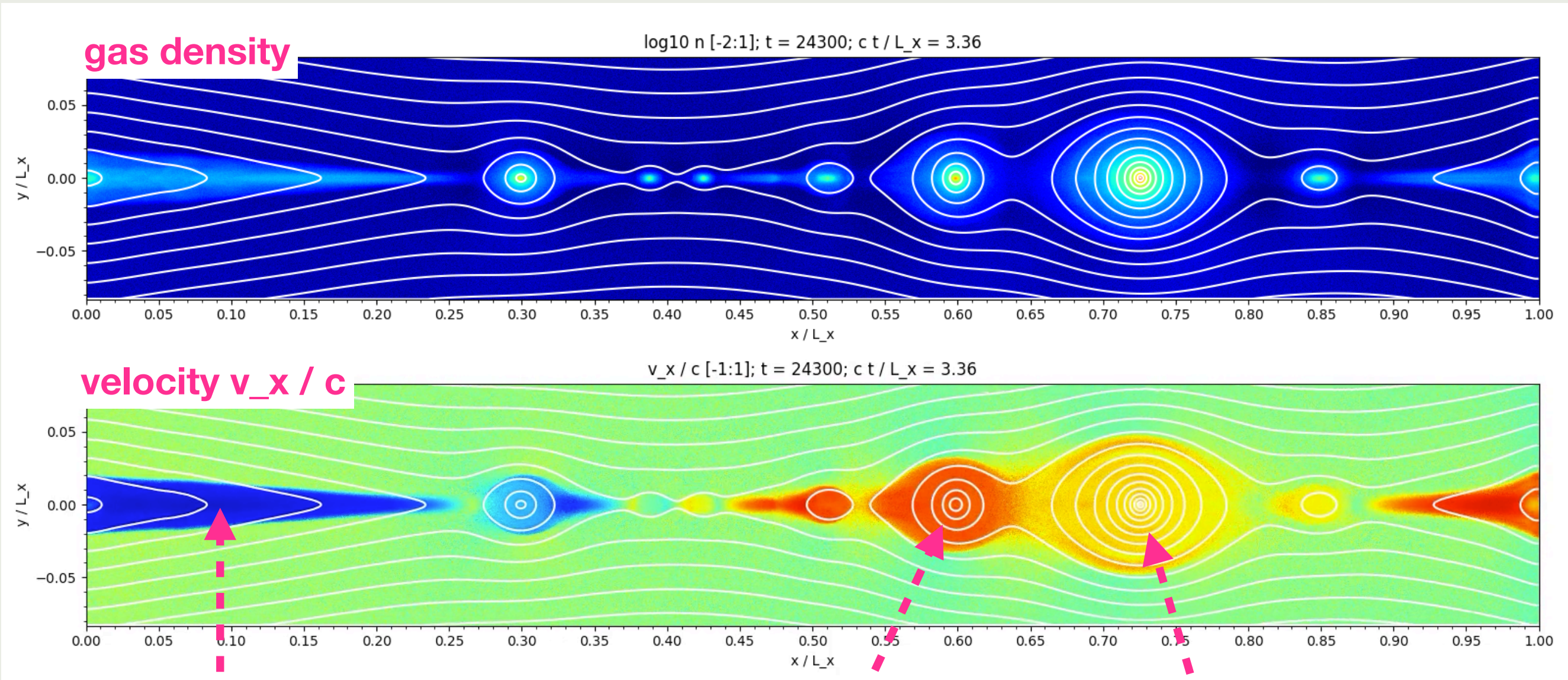
PARTICLE-IN-CELL SIMULATION OF RELATIVISTIC RECONNECTION WITH OPEN BOUNDARIES



J. Ortuño-Macías & KN (2020)

see also
Daughton et al. (2006)
Sironi et al. (2016)

PARTICLE-IN-CELL SIMULATION OF RELATIVISTIC RECONNECTION WITH OPEN BOUNDARIES



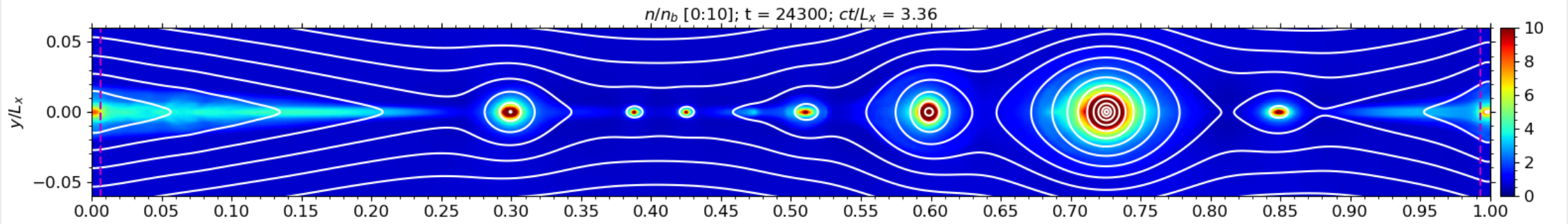
minijet

small/fast
plasmoid

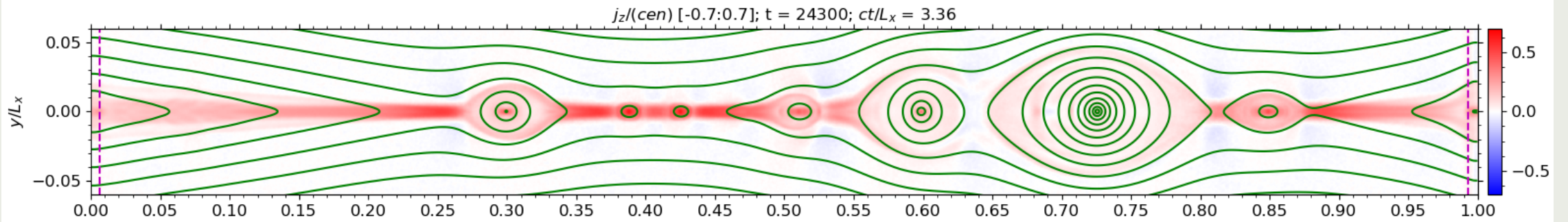
large/slow
plasmoid

J. Ortuño-Macías & KN (2020)

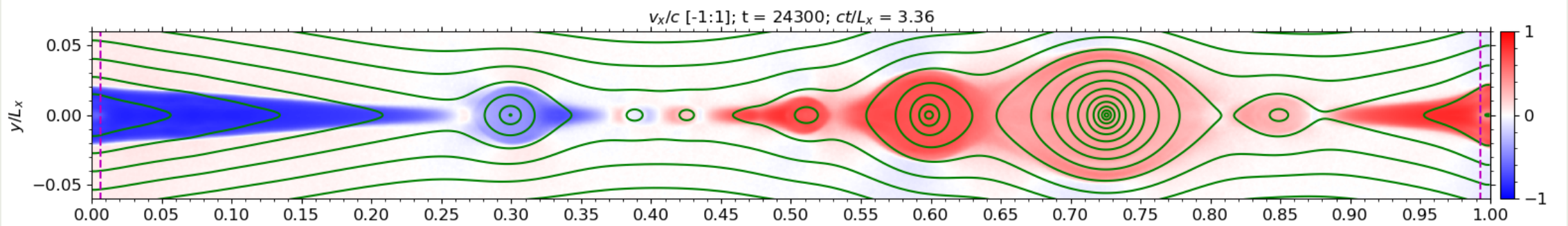
gas
density



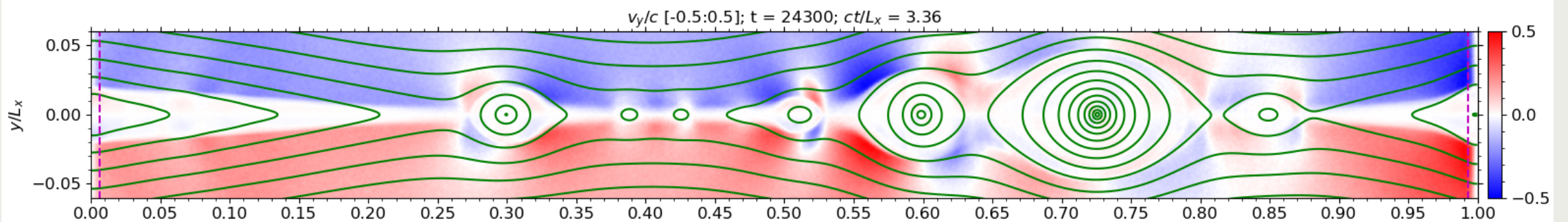
current
density



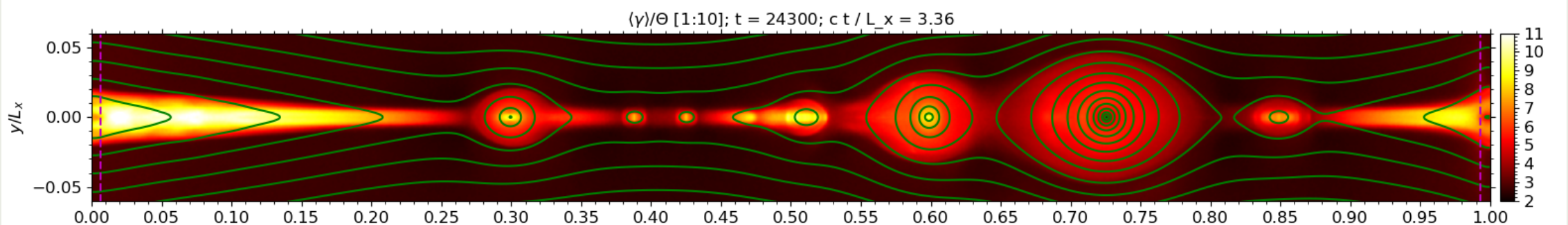
horizontal
velocity



vertical
velocity



mean
particle
energy



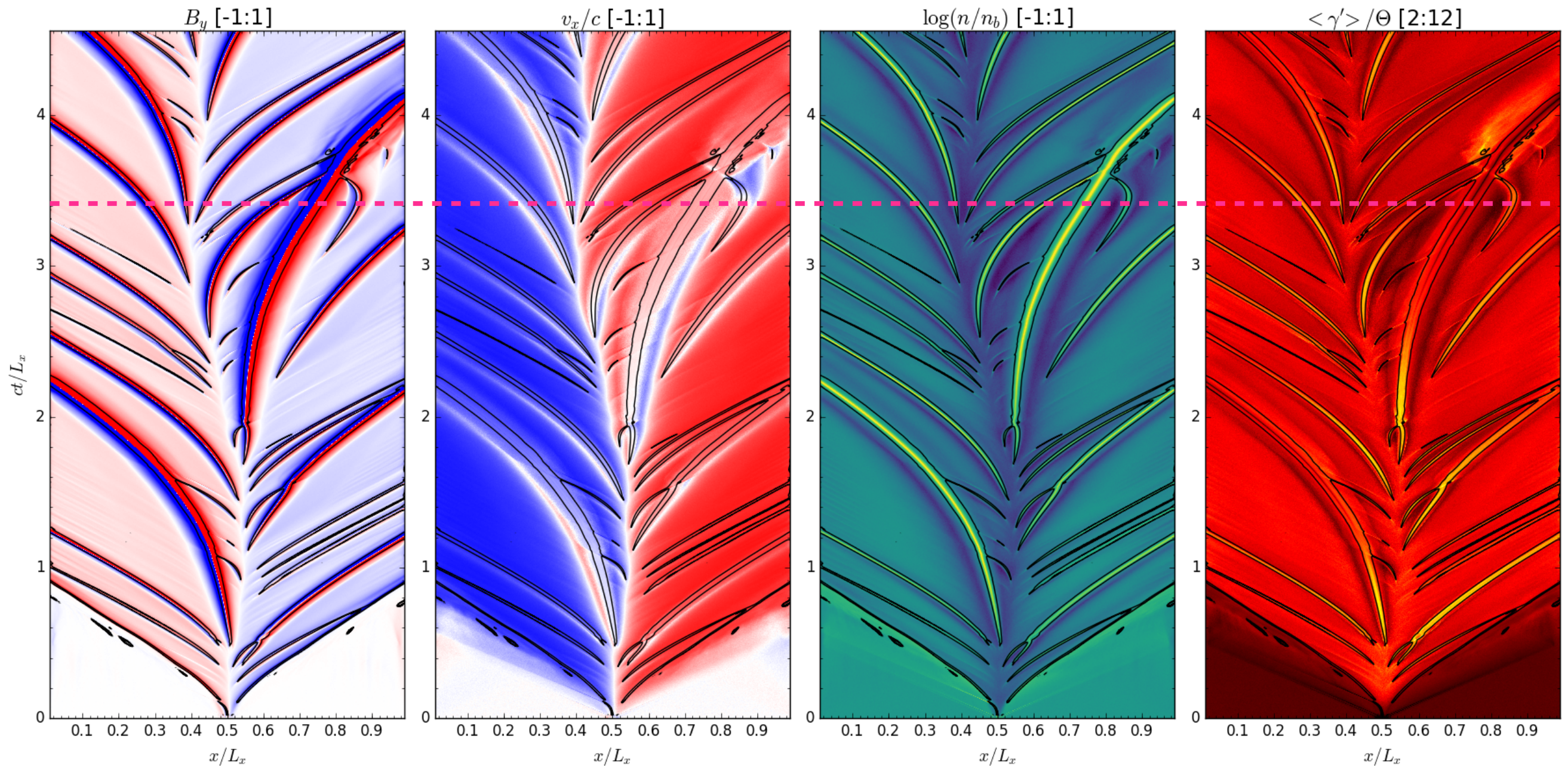
RECONNECTION WITH OPEN BOUNDARIES: SPACETIME DIAGRAMS

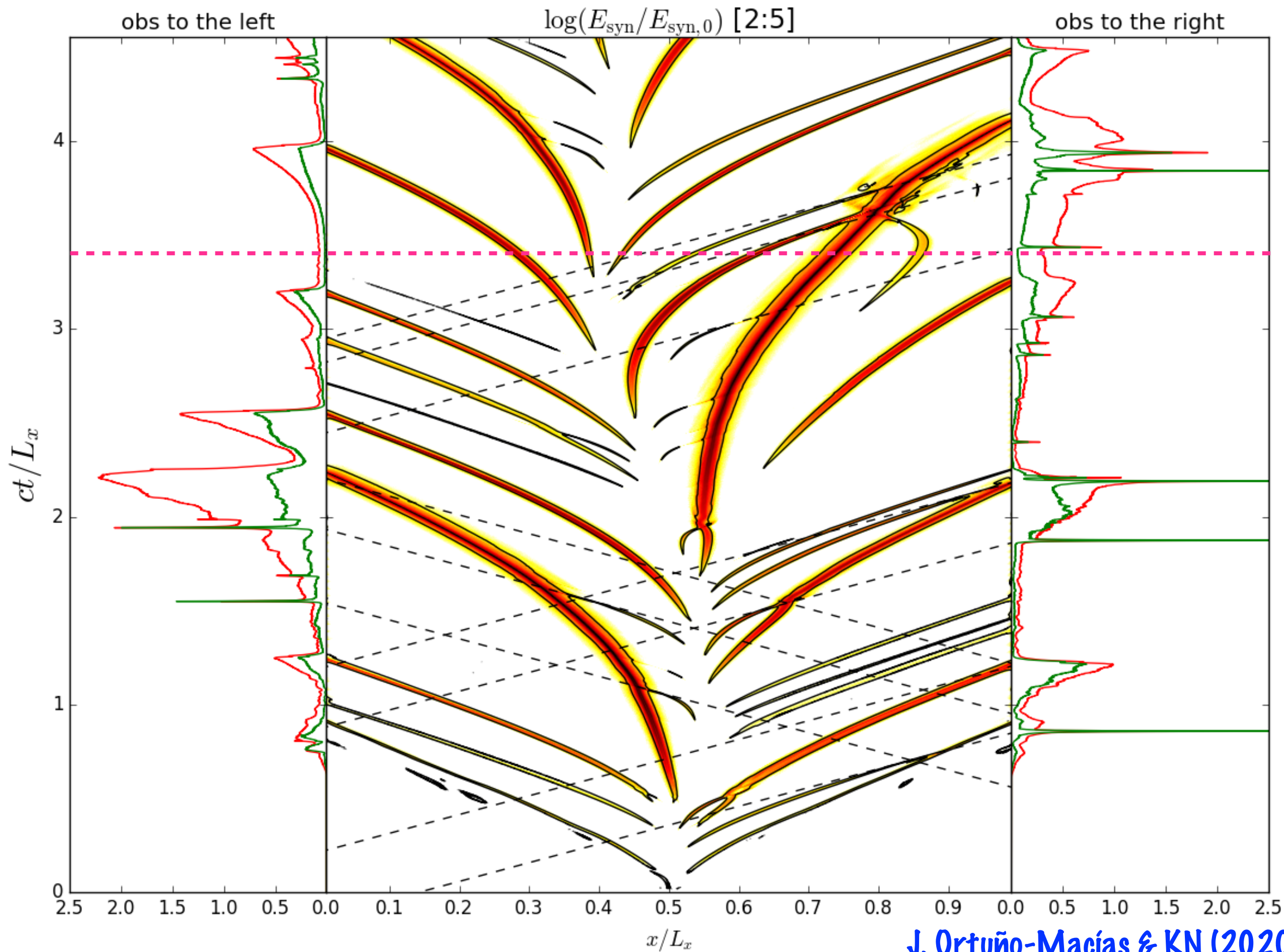
magnetic field B_y

velocity v_x

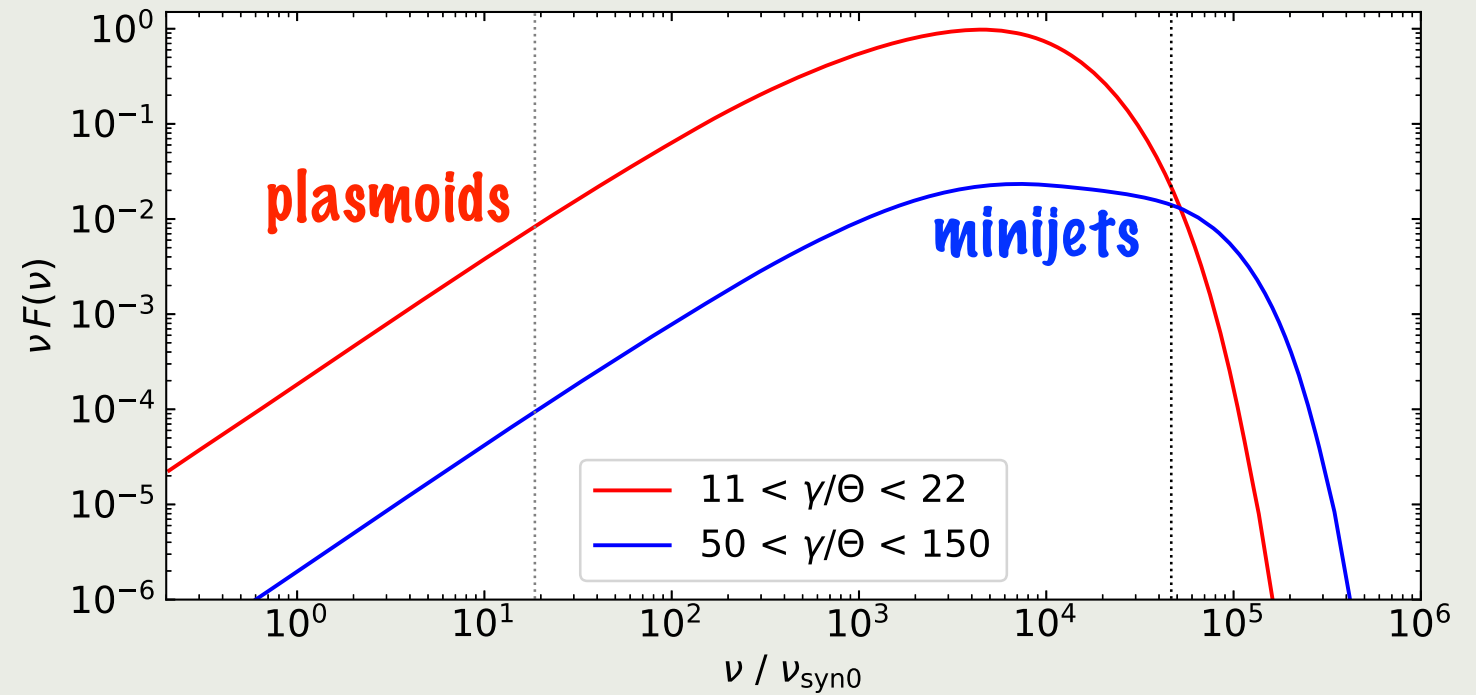
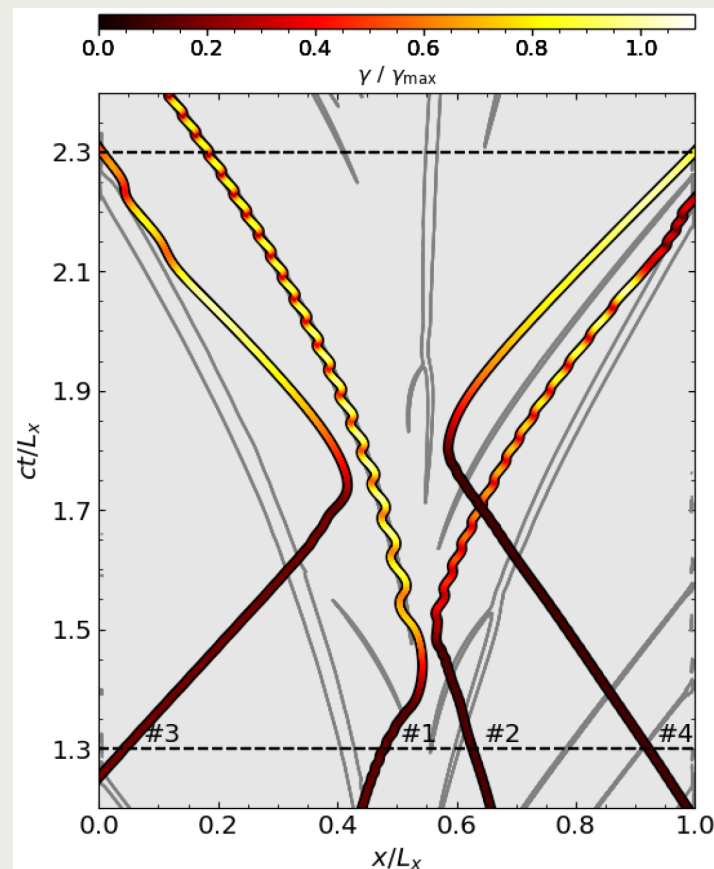
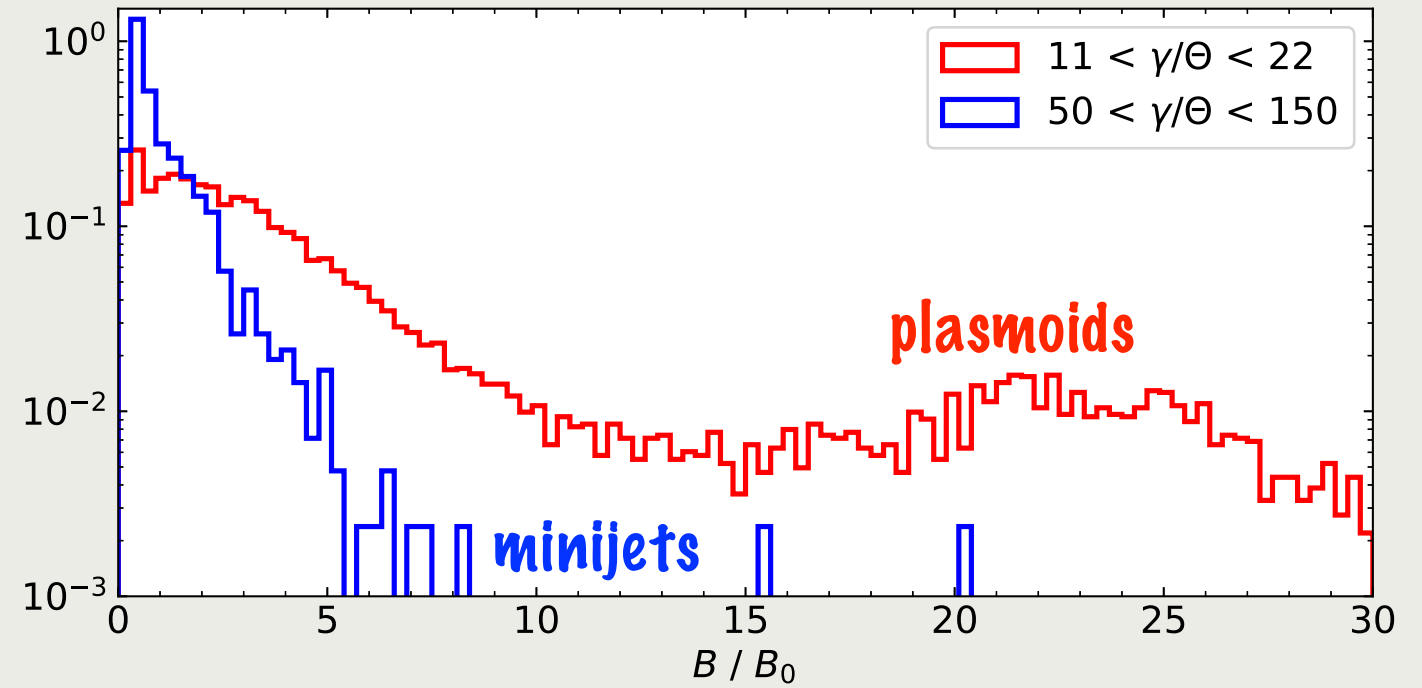
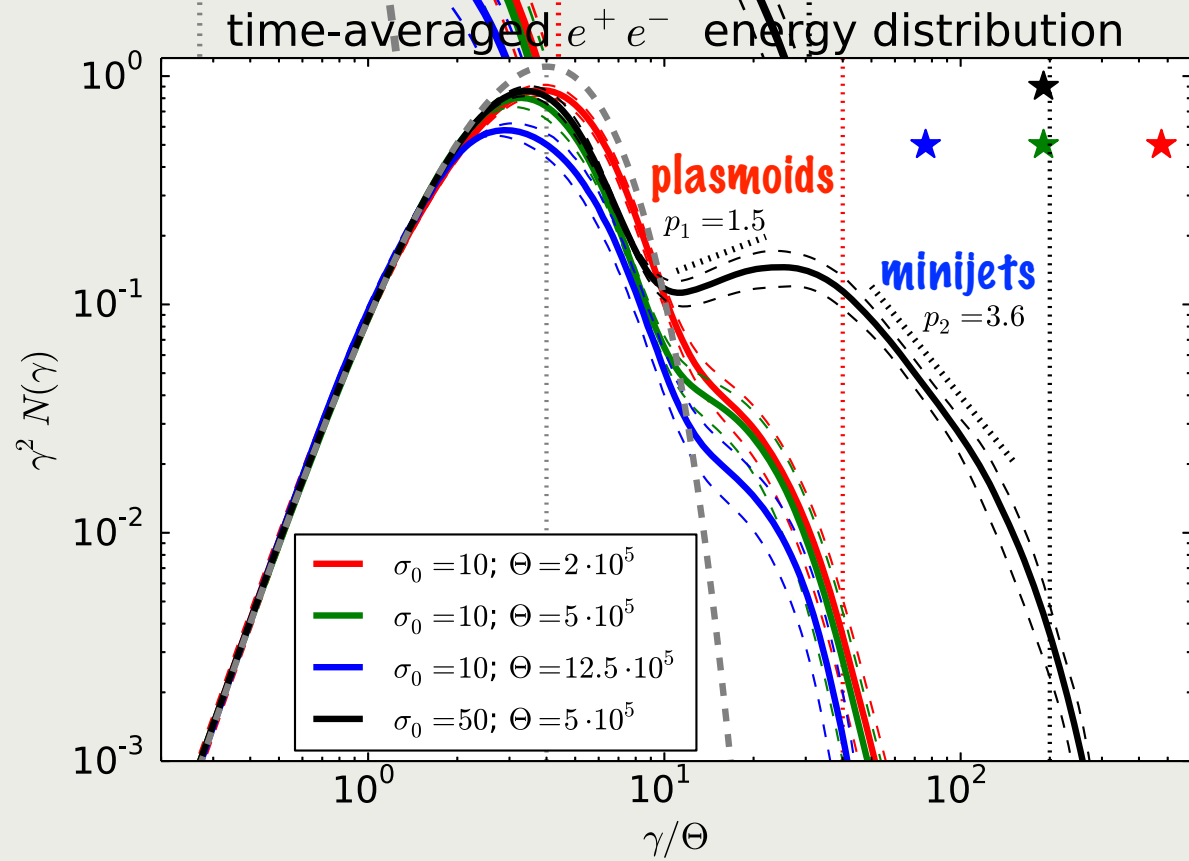
gas density

mean particle energy
in co-moving frame





PARTICLE ACCELERATION: PLASMOIDS VS MINIJETS



SUMMARY

- Magnetic reconnection is a change in the topology of reversed magnetic field lines that allows to convert magnetic energy to heat, motion and non-thermal particle acceleration.
- The basic Sweet-Parker model based on uniform magnetic diffusivity is very inefficient due to low reconnection rate (inflow velocity $v_{\text{in}} \ll c$).
- Localized diffusivity (Petschek model) and production of plasmoid chains (tearing instability) make reconnection efficient ($v_{\text{in}} \sim 0.1c$).
- Particles can be accelerated at multiple locations in the reconnection layer: magnetic X-points, plasmoids, plasmoid mergers.